Journal of Inorganic and Organometallic Polymers and Materials (2023) 33:3894–3914
https://doi.org/10.1007/s10904-023-02672-2

RESEARCH

Effectiveness of Silicon Dioxide Nanoparticles (Nano SiO_2) on the Internal Structures, Electrical Conductivity, and Elevated Temperature Behaviors of Geopolymer Concrete Composites

Hemn Unis Ahmed[1,2] · Azad A. Mohammed[1] · Ahmed Salih Mohammed[1]

Received: 21 March 2023 / Accepted: 20 April 2023 / Published online: 11 May 2023

Abstract
The swift growth of urban areas and industries has resulted in a rise in concrete production and subsequent depletion of resources as well as environmental pollution. In light of environmental considerations, it has become imperative to discover and advance alternative binding construction materials that can substitute conventional Portland cement. Geopolymers have emerged as a viable solution to this issue. Geopolymer composites can benefit from unique attributes and improved performance through the use of nanomaterials. This is achieved by augmenting the composite's microstructural features, creating additional C-S-H, N-A-S-H, and C-A-S-H gels, and filling in nanopores within the matrix. In this paper, extensive experimental laboratory works have been conducted to investigate the effects of adding different dosages (1, 2, 3, and 4%) of nano-silica (NS) particles on the setting times, compressive strength, splitting tensile strength, resistance to elevated temperatures, electrical resistivity, bulk electrical conductivity, thermogravimetric analysis and scanning electron microscopy of geopolymer concrete composites. As a result of the addition of NS, the mechanical strength, electrical conductivity, and thermal behavior of geopolymer concrete all improved by 21%, 36%, and 26%, respectively, in comparison to the control GPC mixture. Furthermore, according to SEM observations, the addition of NS improved the microstructural characteristics of the GPC specimens due to the formation of additional geopolymerization products. Finally, it was discovered through statistical and multivariate analysis that the developed model codes, such as ACI 318, ACI 363, AS3600, and CEB-FIP, are not suitable for predicting splitting tensile strength, electrical resistivity from their tested compressive strength values.

Keywords Geopolymer concrete · Setting times · Mechanical properties · Elevated temperature · Electrical conductivity · Microstructural analysis

1 Introduction

There is a growing need for concrete worldwide to keep up with the rising demand for infrastructure. Recently, Ordinary Portland cement (OPC) is commonly used as the binding material for concrete. Nevertheless, the production of cement leads to significant greenhouse gas emissions [1]. The cement industry is one of the largest emitters of carbon dioxide (CO_2), accounting for approximately 5–8% of total global emissions [2]. Additionally, the production of cement clinkers, a key component of cement, requires significant amounts of raw materials such as limestone and shale, with estimating that it takes around 2.8 tons of these materials to produce one ton of cement [3]. Despite these environmental impacts, Portland cement has remained the primary binding material for manufacturing concrete composites [4]. This is largely due to its affordability, availability, and compatibility with existing infrastructure and construction practices.

However, there has been a growing interest in developing more sustainable alternatives to Portland cement, such as geopolymer concrete, which is made by combining industrial byproducts with alkaline activators. Geopolymer concrete offers a range of benefits over traditional concrete, including superior mechanical properties, durability,

✉ Hemn Unis Ahmed
hemn.ahmed@univsul.edu.iq

[1] Civil Engineering Department, College of Engineering, University of Sulaimani, Sulaimaniyah, Kurdistan Region, Iraq

[2] Civil Engineering Department, Komar University of Science and Technology, Sulaimaniyah, Kurdistan Region, Iraq

and resistance to acid and sulfate attacks, as highlighted by Provis and Bernal [5].

Geopolymers are a type of inorganic material produced by activating alkaline substances with a source of binder material rich in aluminum and silicates. These binder materials can include fly ash and ground granulated blast furnace slag (GGBFS) [6]. According to Ahmed et al. [7], the components of geopolymer concrete are similar to those of traditional concrete composites, consisting of aggregates, alkaline solution, and source binder materials. The polymerization reaction between the alkaline solution and source binder materials results in the formation of geopolymer concrete, much like the process of forming conventional concrete composites. Mohammed et al. [8] have pointed out that several factors, such as the ratio of sodium silicate to sodium hydroxide, sodium hydroxide concentration, the ratio of alkaline solution to source binder materials, curing conditions, the amount of additional water and superplasticizers, the chemical composition and quantity of source binder materials, and the quality and type of aggregates, play a crucial role in determining the characteristics and behavior of geopolymer concrete. To accelerate the polymerization process and achieve the desired mechanical and physical properties of geopolymer concrete, scholars have utilized heat-curing methods. However, this approach has limitations, as it restricts the use of geopolymer concrete in on-site engineering projects and limits the use of geopolymer concrete in precast concrete elements, as noted by Hassan et al. [9]. In response, Ahmed et al. [10] have suggested the use of nanoparticles (NPs) as an alternative approach to produce geopolymer concrete with ambient curing conditions.

According to Sharif [11], the field of nanotechnology in civil engineering is still in its nascent stage. However, various types of nanomaterials have demonstrated significant benefits over other additives in geopolymer concrete (GPC) composites, such as improved mechanical properties and enhanced long-term durability. Nanotechnology refers to the application of science, engineering, and technology at a scale ranging from 1 to 100 nm (nm), as defined by convention. This scale is larger than individual atoms, which are typically around 0.2 nm in size but smaller than the point at which nanomaterial-related phenomena can be observed [12]. The unique characteristics of NPs, such as their high reactivity and surface area-to-volume ratio, make them highly effective at modifying the microstructure of GPC. By altering the atomic-level structure, NPs have the potential to significantly enhance the performance and properties of geopolymer composites in both the fresh and hardened states. In particular, the addition of NS to geopolymer concrete has been shown to increase the dissolving rate of Si and Al, which in turn influences the polymerization process and leads to improved performance [13].

According to Faraj et al. [14], nano-silica (NS), a type of amorphous silica with nanometer-scale particle size, has gained popularity in the construction industry. This is due to its exceptionally high surface area, which enables it to enhance concrete properties by promoting the formation of additional C-S-H gels during the pozzolanic reaction and acting as nano-fillers in the concrete pores. Behfarnia and Rostami [15] conducted a study on how the addition of micro and nano-silica impacted the permeability of geopolymer concrete made with GGBFS. They discovered that replacing some of the GGBFS with NS had a negative effect on the paste's microstructure, resulting in inadequate permeability outcomes. However, using micro silica improved the permeability of the geopolymer concrete specimens. Similarly, the mechanical and microstructural properties of geopolymer concrete composites made from blended fly ash and GGBFS were enhanced by adding micro and nano-silica, as reported by Mustakim et al. [16]. Furthermore, Çevik et al. [17] conducted experiments and found that incorporating NS into geopolymer concrete mixtures made from fly ash improved the durability, residual mechanical strength, and mechanical performance in chemical environments. The addition of NS reduced porosity and a denser structure of the specimens, resulting in these positive effects. Also, Ibrahim et al. [82] conducted a study to investigate how the addition of NS affected the strength and microstructure of geopolymer concrete. Their findings revealed that the nano-geopolymer concrete mixtures' compressive strength and microstructural properties were significantly better than those of the reference specimens.

The impact of incorporating hybrid nano-clay (NC) and carbon nanotubes (CNT) on the engineering properties of geopolymer concrete composites was examined by Kotop et al. [18]. The results showed that the geopolymer mixture that had 2.5% NC along with 0.01% CNTs produced the highest compressive strength in the geopolymer concrete specimens. On the other hand, Saini and Vattipalli [19] conducted experiments to determine the optimal mixture for GGBFS-based geopolymer concrete. Their findings showed that a mixture with a sodium hydroxide molarity of 16 M, a binder content of 500 kg/m3, and 2% NS at 90 days of age resulted in the highest compressive strength, flexural strength, and splitting tensile strength when compared to other mixture combinations.

In addition, Shahrajabian and Behfarnia [20] conducted a study to investigate the effect of nano-silica, nano-alumina, and nano-clay on the freeze–thaw resistance of geopolymer concrete. Their results determined that adding NS and nano-clay was more effective than nano-alumina in improving the strength and durability of the geopolymer concrete specimens that underwent freeze–thaw cycles. Moreover, Alzeebaree [21] found that adding nano-silica and metakaolin had an adverse effect on the fresh properties of GGBFS-based

self-compacting geopolymer concrete. However, the same study showed that including these materials improved properties such as compressive and bond strength, fracture energy, and stress intensity factor. A similar outcome was observed by Mohammedameen [22] for fly ash-based self-compacting geopolymer concrete.

Ahmed et al. [23] noted that in previous studies, fly ash was frequently utilized as the primary aluminosilicate source. Numerous experiments have been conducted to substitute fly ash with GGBFS in geopolymer concrete, resulting in improved mechanical performance. However, a dearth of studies thoroughly investigate the properties of GGBFS as the sole binder ingredient in geopolymer concrete with various doses of nano-silica. Thus, the aim of this study is to extensively examine the impact of nano-silica on several properties of GGBFS-based geopolymer concrete, including setting time, compressive strength, splitting tensile strength, resistance to elevated temperatures, bulk electrical conductivity, electrical resistivity, and microstructural characteristics (such as SEM and TGA), through extensive laboratory experimentation.

2 Experimental Program and Methodology

2.1 Materials

Ground granulated blast furnace slag (GGBFS) was used as the main source binder materials for manufacturing geopolymer concrete mixtures. The physical and chemical characteristics of GGBFS are given in Table 1. Also, the geopolymer concrete mixtures used a constant percent of about 10% of the total binder content of silica-fume. The physical and chemical characteristics of silica-fume (SF) are given in Table 1. Moreover, hydrophilic NS particles in the powdered form were obtained from LUOYANG company in china. The extremely small nanoparticles (NPs) of NS, which are in the range of 30 nm, can significantly enhance the performance of GPC mixtures. The physical and chemical characteristics of NS particles are provided in Table 1. A commercially available superplasticizer named Hyperplast PC900 from a DCP company with a slump retention capacity. This superplasticizer complies with ASTM C494, TYPE G, with a specific gravity of 1.12 g/cm^3 and a pH value of 5 to 7.

Furthermore, well-graded crushed coarse and natural river fine aggregates were used, with a specific gravity of 2.69 and 2.7, respectively. The maximum size of the coarse aggregate was 12.5 mm, and water absorption was 1.37%, while the water absorption of the fine aggregate was 1.73%. The gradation of fine and coarse aggregate are presented in Fig. 1a and b, respectively. Regarding the alkaline solution, a combination of 12 M sodium hydroxide (NaOH) and sodium silicate (Na_2SiO_3) solutions is consumed as the alkaline liquid for geopolymer concrete mixtures. Both were obtained from the Malbray chemical factory in Erbil, Kurdistan Region, Iraq (36°10′03.6″N, 44°00′41.1″E). The NaOH was in pellet form with 98% purity, while sodium silicate was in a liquid form consisting of 37.5% SiO_2, 16.5% Na_2O, and 46% H_2O. The specific gravity of sodium silicate and sodium hydroxide was 1.5 and 1.34, respectively. Table 2 shows the chemical compositions of both NaOH and Na_2SiO_3.

Table 1 Chemical compositions and physical properties of GGBFS, SF, and NS

Elements	GGBFS Wt%	SF	NS
Na_2O	1.7800	–	–
MgO	6.675	0.33	0.004
Al_2O_3	11.641	–	–
SiO_2	38.159	92.4	99.5
SO_3	1.93	–	–
K_2O	0.8045	–	–
CaO	30.966	0.143	0.008
TiO_2	1.51	–	–
Fe_2O_3	1.591	0.13	0.007
MnO	2.295	–	–
Ba	0.517	–	–
Sr	0.07	–	–
Cu	0.07	–	–
LOI	2	7	–
Specific gravity(g/cm^3)	2.9	2.25	0.7
Blaine fineness	5800 (cm^2/g)	–	185 ± 20 (cm^2/g)
Bulk Density	–	650 (kg/m^3)	0.18 (g/cm^3)

2.2 Mix Proportions

Five geopolymer concrete mixtures have been prepared with different NS dosages (0, 1, 2, 3, and 4%). The mix design procedures have been carried out by benefiting from Reddy et al. [24] and Li et al. [25]. The concrete mixture proportions should be balanced between economy and workability, strength, durability, density, and appearance criteria. The first stage contained five mixes, including the control mixture. Four different percentages of NS particles were used as the total binder content replacement, including 1%, 2%, 3%, and 4% by weight of the total source binder materials. The mix names can be explained as follows: G1 is the control mixture with 0% of NS particles, and G2 stands for 1%. The same designation sequence is applied to other mixes. Table 3 reports the mix proportions for all mixes.

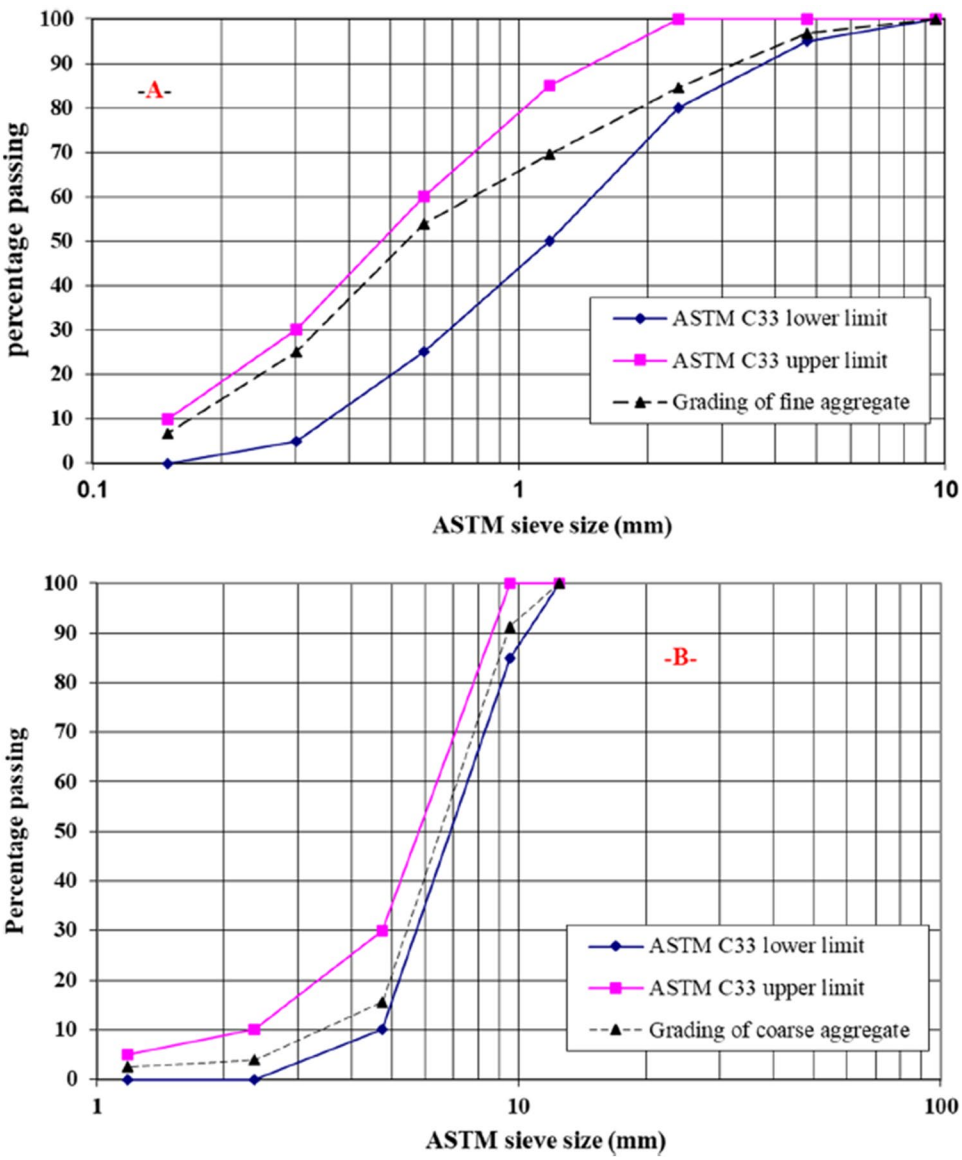

Fig. 1 Sieve analysis aggregates **a**: fine aggregate, **b** coarse aggregate

Table 2 Properties of sodium hydroxide and sodium silicate

Elements	NaOH	Na_2SiO_3
Physical state	Solid	Liquid
Appearance	White	viscous clear to light yellow liquid
Sodium hydroxide (NaOH)	98%	–
Sodium carbonate (Na_2CO_3)	1%	–
Silicate (SiO_2)	0.05%	37.5%
Sodium chloride (NaCl)	0.036%	–
Copper	2 ppm	–
Sodium Sulfate (Na_2SO_4)	0.045%	–
H_2O	–	46%
Na_2O	–	16.5%

2.3 Mixing and Casting

The mixing sequence and duration are very important in GPC production. For this reason, constant mixing and the batching procedure were followed in this study to obtain the same homogeneity and uniformity in all mixtures. Regarding the procedure, in the first stage, the granular materials, such as fine aggregates and coarse aggregates, were poured into a power-driven revolving pan mixer and mixed homogeneously for 30 s. Afterward, the powdered materials (GGBFS and silica fume and NS particles), drily mixed previously in a suitable container, were added to the mixer and mixed with aggregates for about 60 s in the second stage. Afterward, in the third stage, the alkaline solution (prepared 24 h before mixing) and a mixture of extra water and superplasticizer (also mixed previously) were poured into the concrete mixer

Table 3 GPC mix proportions in kg/m^3

Mix ID	GGBFS	SF	NS	SH	SS	EW	SP	FA	CA
G1	400	50	0	64.3	160.7	24.75	9.45	612.28	1104.27
G2	395.5	50	4.5	64.3	160.7	24.75	9.45	607.55	1095.72
G3	391	50	9	64.3	160.7	24.75	9.45	602.82	1087.2
G4	386.5	50	13.5	64.3	160.7	24.75	9.45	598.10	1078.67
G5	382	50	18	64.3	160.7	24.75	9.45	593.37	1070.14

GGBFS Ground granulated blast furance slag; *SF* Silica-fume, *NS* nano-silica, *SH* Sodium hydroxide, *SS* Sodium silicate, *EW* Extra water, *SP* Superplastisizer, *FA* fine aggregate, *CA* Coarse aggregate

slowly, followed by 180 s of mixing. After the mixing procedure was finished, several samples were cast inside the required molds with lubricating surfaces to test the GPC mixes' different properties. A vibrating table made GPC denser air bubbles as the fresh concrete was poured into the molds. The specimens were taken out of the mold after 24 h and allowed to cure in the lab at 23 ± 2 °C until they were ready for testing.

2.4 Test Setup

The compressive strength measurement of GPC mixtures, 100×200 mm cylindrical samples were tested concerning ASTM C39 utilizing a 3000 kN capacity universal testing compression machine. The test is conducted on three samples from each GPC mix at 3, 7, 28, 90, and 180 days. The specimens were loaded at a stress rate of 0.25 MPa/s. The compressive strength was computed by averaging the results from the three tested samples at each testing age. The surface of the specimens was capped using sulfur mortar according to ASTM C617. Table 4 lists all the other geopolymer concrete tests conducted for this investigation applying their standard test methods.

3 Results and Discussions

3.1 Initial and Final Setting Time

Figure 2 depicts the effects of varying NS contents on the initial setting time (IST) and final setting time (FST) of geopolymer paste composites. It can be seen that adding NS to the geopolymer paste mixtures leads to an increase in both IST and FST. For example, the value of IST was 17, 19, 21, 24, and 25 min at 0, 1, 2, 3, and 4% of NS dosages, respectively. These results demonstrated that adding NS to the GGBFS-based geopolymer pastes increased the initial setting time by 11.76%, 23.53%, 41.18%, and 47.06% at the loading rate of NS content by 1, 2, 3, and 4%, correspondingly, compared to the virgin GGBFS-based geopolymer paste mixture without any dosages on NS content as presented in Fig. 2. Similarly, based on the experimental results, the final setting time increased as the dosage of NS increased in the GGBFS-based geopolymer paste system. The FST for the loading rate of 0, 1, 2, 3, and 4% NS were 27, 29, 32, 34, and 37 min, respectively, which is comparable to the increase in FST by 7.41%, 18.52%, 25.93%, and 37.04% for 1, 2, 3, and 4% NS content, respectively, relating to the control geopolymer paste mixture. The reason for these results was thought to be that when NS was added to the geopolymer paste mixture, the amount of silica in the mixture went up. As a result, more silicate oligomers were made, and changing this product into a polymer network takes a long time; this issue leads to delays in the geopolymer paste's initial and FST [26]. The findings of this study are analogous to those of Mustakim et al. [16] investigated the effects of micro- and nano-silica addition on the mechanical, microstructural, and fresh characteristics of blended FA/GGBS-based geopolymer concrete. They discovered that compared to the control geopolymer mixture that lacked any NS or micro-silica components, both NS and micro-silica increased the initial and FST of the geopolymer paste. For

Table 4 Tests and standard test methods followed in this study

NO	Tests	Standard test methods	Test date (Days)
1	Initial and final setting time	ASTM C642	–
2	Compressive strength	ASTM C39	3, 7, 28, 90, 180
3	Electrical resistivity	ASTM G57	90
4	Bulk electrical conductivity	ASTM C1760	90
5	Elevated temperature behaviors	ISO 834 and RILEM	28
6	Scanning electron microscopy	–	28
7	Thermogravimetric analysis	–	28

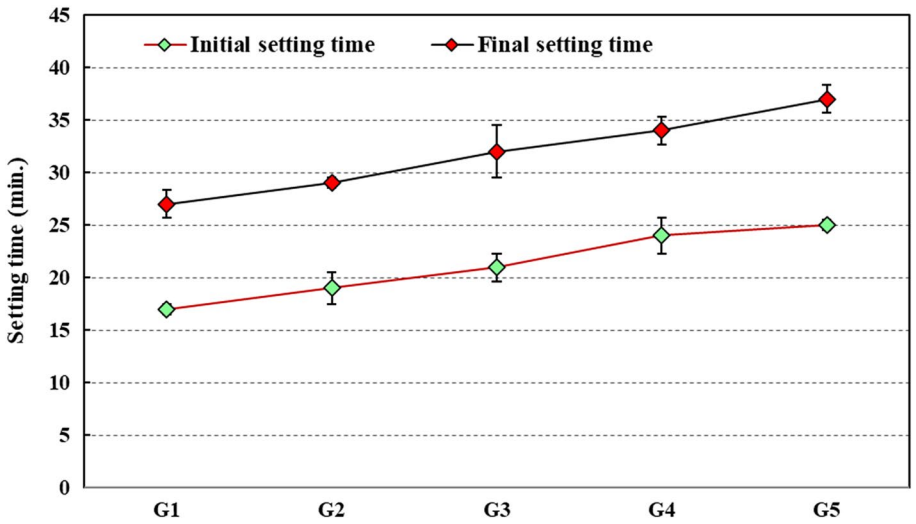

Fig. 2 Setting time of GP paste with different dosages of NS

instance, the initial and FST increased by 16.7% and 25%, respectively, compared to the control combination at the dosage of 1.5% NS. This increase was simultaneously 12.5% and 15.4% when micro-silica was added to the mixture [16]. Also, Huseien et al. [27] and Samadi et al. [28] observed that adding waste glass nanopowders increased the initial and FST of blended GGBFS/FA-based geopolymer mortar. Moreover, Gao et al. [29] discovered that increasing the NS dose from 0 to 3% raised the initial/FST of the geopolymer paste with a slag/fly ash ratio of 70/30 from 27/71 min to 37/85 min, while samples with a slag/fly ash ratio of 30/70 rose from 76/128 min to 96/154 min.

3.2 Compressive Strength

Compressive strength is considered one of the most important mechanical properties of concrete, as it provides an overall indication of the concrete's quality and structural performance. This property is frequently used to evaluate the suitability of concrete for various applications, including construction of buildings, bridges, and highways. Compressive strength is also used to measure the effectiveness of concrete mixtures in resisting external forces, such as those generated by wind, earthquakes, or heavy loads. Therefore, it is crucial to investigate the factors that influence compressive strength and to develop techniques to enhance it.

The influence of incorporating NS on the compressive strength of GGBFS-based geopolymer concrete was evaluated by measuring the compressive strength at 3, 7, 28, 90, and 180 days of age. The results showed that the addition of NS to GGBFS-based geopolymer concrete mixtures enhances the compressive strength at all ages compared to the control concrete specimens. The compressive strength of geopolymer concrete increased as the age of the samples increased. However, the increase was more significant at early ages than later. For example, mix G4 showed a 32.2% increase in compressive strength between 3 and 7 days, a 45.9% increase between 7 and 28 days, a 10.9% increase between 28 and 90 days, and a 2.3% increase between 90 and 180 days. Similar trends were observed in other geopolymer concrete mixtures, even when different dosages of NS were used. This result emphasizes that most of the polymerization process and formation of hydration products occurred in the early ages [17, 30]. On the other hand, the compressive strength of the concrete specimens was increased as the NS dosages increased to 3%, then slightly decreased in all ages, as shown in Fig. 3. At the age of 3 days, the compressive strength improved by 3.42, 5.14, 6.29, and 5.71% at the 1, 2, 3%, and 4% dosages of NS, correspondingly, compared to the reference concrete mixture; while, this improvement in the compressive strength rose as the age of the geopolymer concrete increased. For example, at 28 days, the compressive strength was enhanced by 9.4, 14.43, 20.47, and 12.1% at 1, 2, 3, and 4% dosages of NS, respectively, respectively, compared to the control geopolymer concrete specimen without any dosages of NS. Alternatively, about 10.18%, 14.97%, 21.86%, and 14.37% increment in compressive strength was observed for 1%, 2%, 3%, and 4% NS content, respectively, at the age of 180 days. The improvement in the compressive strength of different source binder material-based geopolymer concrete composites were also reported in the literature when different dosages of NS have introduced to the geopolymer concrete mixtures [19, 31–36].

Referring to Fig. 3, it is concluded that the optimum dosages of NS for getting the highest compressive strength of GGBFS-based geopolymer concrete were 3%. Similar results have been reported in the literature by Behfarnia and Rostami [15] and Naskar and Chakraborty [37], however, Alzeebaree [21] and Mohammedameen [22] demonstrated that 2% of NS was the optimum dosage for getting maximum

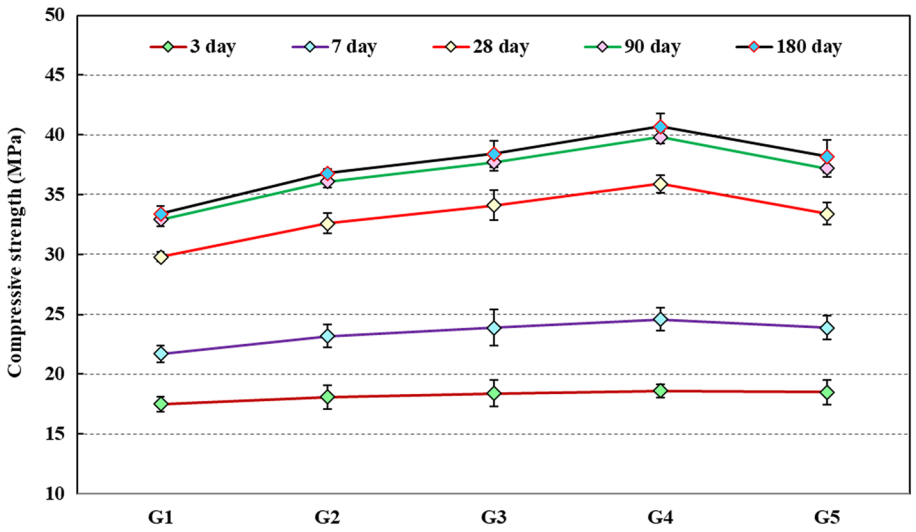

Fig. 3 Compressive strength of GPC mixtures with and without NS

compressive strength of GGBFS and fly ash-based self-compacting geopolymer concrete composites, respectively. On the other hand, Ibrahim et al. [82] reported that a 5% replacement of natural pozzolan with NS gives maximum compressive strength to the natural pozzolan-based geopolymer concrete specimens.

It is well documented in the literature that the reaction mechanism progresses in geopolymers consisting of three major steps. First, the aluminosilicate particles are dissolved in the extremely alkaline activators to create a solution. The concentration of this solution increases over time as the dissolution continues to add silicates to those already present in the alkaline activator, culminating in the development of long chains as oligomers in the gelation process in the second stage. Finally, in the third stage, poly-condensation occurs when aluminosilicate species in the gel continue to rearrange and reorganize themselves to form a bigger network, producing three-dimensional aluminosilicate chains [38]. The remarkable enhancement in the compressive strength of GGBFS-based geopolymer concrete containing NS, as depicted in Fig. 3, especially with 3% NS, could be attributed to the enhanced transformation of source materials to the polymeric gel such as C-S-H, N-A-S-H, and C-A-S-H gels in the presence of highly reactive NS, as well as a possible particle packing effect of nanoparticles in the binder structure by filling nano-pores within the geopolymer concrete matrixes, which, in turn, improves the specimens' strength [15], Ibrahim et al., [82]. on the other hand, the compressive strength reduction was attributed to the matrix's overflowing availability of unreacted NS particles. The excess amount of NS caused agglomerations between the NS particles, which could have prevented silica dissolution, resulting in the formation of voids and, as a result, a decrease in the compressive strength of the geopolymer concrete [16], in addition, poor dispersion of NPs within the concrete mixtures counted as another reason for the decline in the compressive strength [39].

Finally, Fig. 4 depicts the compression failure mode of all GPC mixtures from G1 to G5 with and without varying NS dosages. During the compressive strength tests, visual observations were made, and it was discovered that at ultimate load, there is no significant difference in the failure mode of all GPC mixtures that kept their shapes after failure, exhibiting more like a ductile failure mode rather than a brittle failure mode. Furthermore, it was discovered that adding NS to GPC mixtures slightly caused the specimens to become brittle.

3.3 Splitting Tensile Strength

At ambient curing conditions, the GGBFS-based geopolymer concrete containing various amounts of NS displayed splitting tensile strength values ranging from 3.31 MPa to 4.08 MPa after 28 days and 3.74 MPa to 4.7 MPa after 90 days. The splitting tensile strength of GGBFS-based geopolymer concrete with varying doses of NS was observed to change between 3.31 and 4.08 MPa and 3.74–4.7 MPa at 28 and 90 days of age, respectively, under ambient curing conditions, as shown in Fig. 5. The splitting tensile strength increased with an increase in NS dosage up to 3%, and then it declined. The improvement rate was 8.46%, 16.9%, 23.26%, and 16.31% at NS loading rates of 1%, 2%, 3%, and 4%, respectively, at 28 days of age. At 90 days of age, this improvement in the splitting tensile strength of GGBFS-based geopolymer concrete was increased to 9.63%, 19.52%, 25.67%, and 19.25% for the same previous content of NS, compared to the control geopolymer concrete specimens that did not contain NS. The experimental results suggest that the most effective dosage of NS for achieving the highest splitting tensile strength in GGBFS-based geopolymer

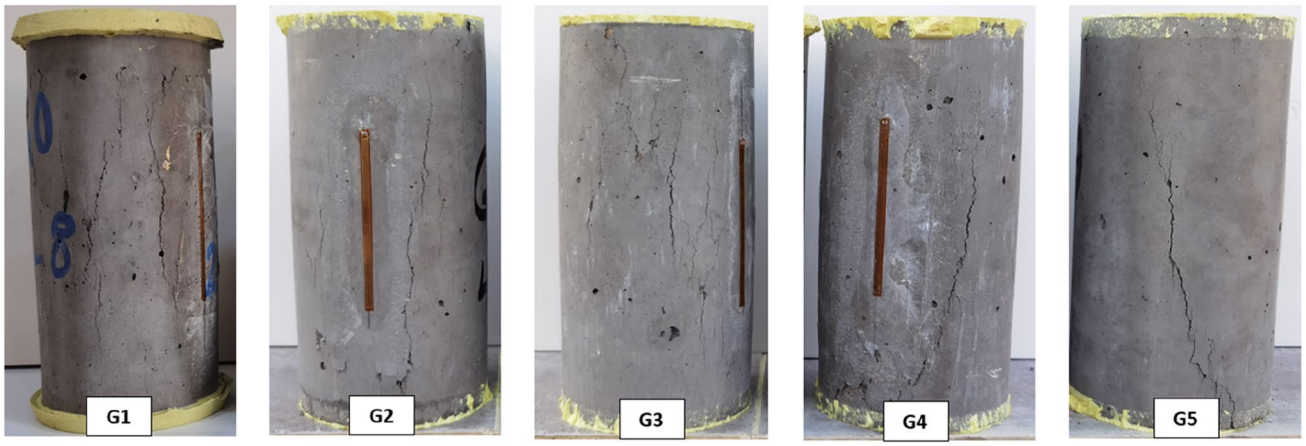

Fig. 4 GPC specimen failure patterns under compression test

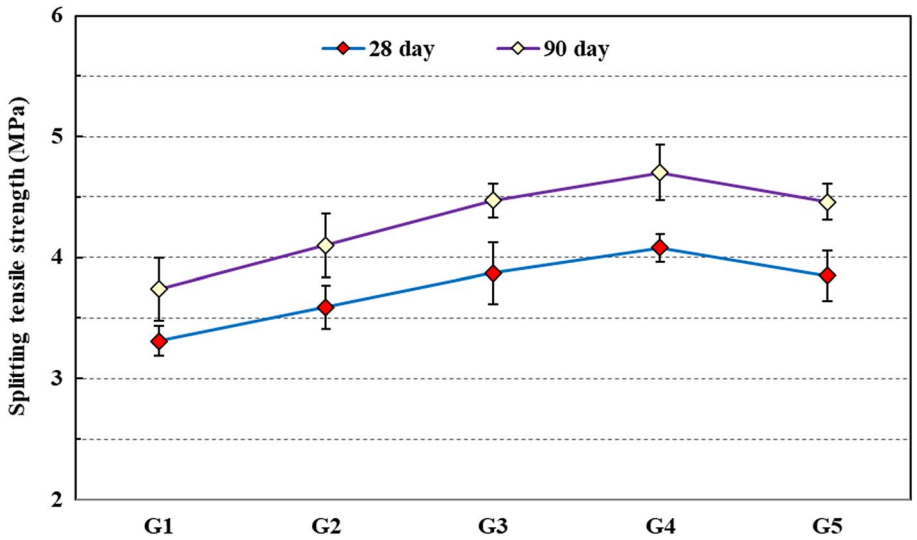

Fig. 5 Splitting tensile strength of GPC mixtures with and without NS

concrete is 3%, which is consistent with the optimal dosage for achieving maximum compressive strength.

The results obtained in this study are consistent with previous findings reported by Mahboubi et al. [40], which showed that the splitting tensile strength of geopolymer concrete was increased by 18%, 30%, and 33% with 1%, 2%, and 3% dosages of NS, respectively, at 28 days of age. Similarly, Nuaklong et al. (2018) found that the splitting tensile strength of geopolymer concrete was improved by 11.1% with the addition of 1.0% of NS compared to the control specimens. Rabiaa et al. [41] discovered that the highest splitting tensile strength was achieved by incorporating 4% of NS into geopolymer concrete mixtures, which was about 21% higher than the control mixture. They also investigated various dosages of NS contents ranging from 0 to 8%. Likewise, previous studies have reported increased the splitting tensile strength of geopolymer concrete when incorporating varying dosages of NS in the mix [32, 42, 43]. As discussed in the section concerning compressive strength, the enhancement in splitting tensile strength within an optimal range of NS and the subsequent decrease in tensile strength beyond this range will be justified similarly.

3.4 Elevated Temperature Behaviours

3.4.1 General Appearance

The visual appearance of GPC specimens under fire exposures of 300 °C, 600 °C, and 900 °C at the age of 28 days is shown in Fig. 6. It is seen that the control samples and those specimens that contained different dosages of NS exhibited slight surface erosion or scaling and roughness with negligible surface spalling. There was no surface erosion for the 300 °C temperature, while the quantity of erosion increased as the temperature increased from 600 °C to 900 °C. Specimens of geopolymer concrete made from GGBFS that lacked

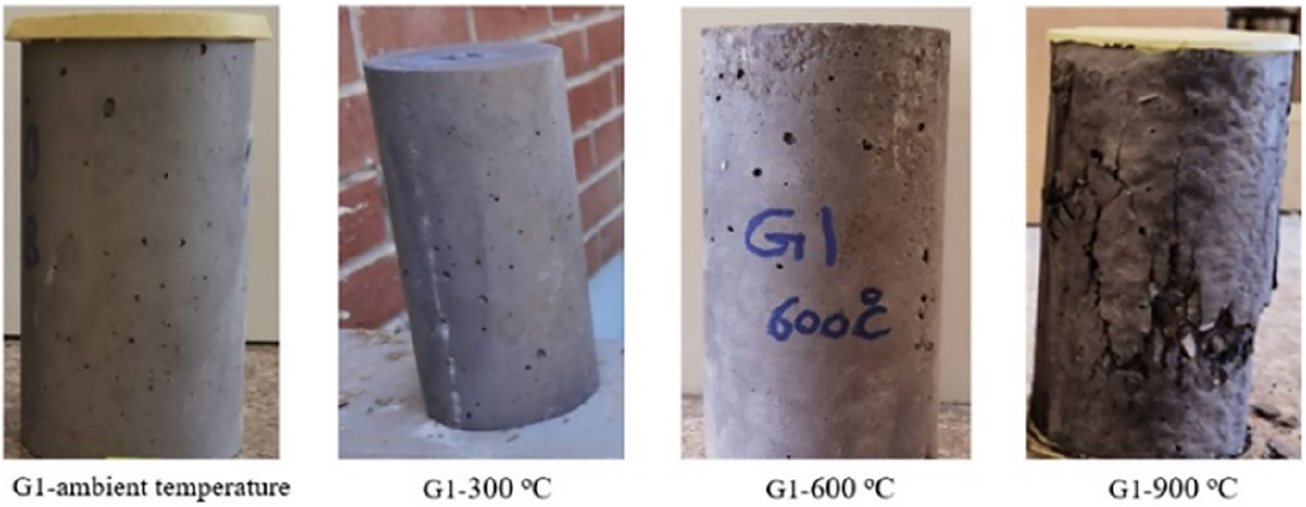

Fig. 6 Visual appearance of various GPC specimens after being exposed to different elevated temperatures

nano-silica exhibited somewhat higher surface degradation than those that contained nano-silica. Also, no significant difference in appearance was observed, and the surface colour was slightly changed from the characteristic grey to light grey. Similarly, it was reported by Nazari et al. [44] that above 600 °C, the color of geopolymer concrete specimens changed to brown colour through the heating process. Also, it was concluded that as the heating temperature rises, the geopolymer concrete specimens get darker [44, 45]. Due to the amount of iron in the matrix and how much it has been oxidized, heat changes the color of geopolymer [46].

3.4.2 Weight Loss

The weight losses of the exposed concrete sample were measured. The mass loss was calculated by weighing the exposed specimens before and after heating. Figure 7 shows the results of the weight loss of geopolymer concrete at 28 days old after incorporating various NS dosages. It is seen that the weight loss of geopolymer samples decreased as the dosages of NS increased, while the weight loss of geopolymer concrete specimens increased as the temperature increased from 300 °C to 600 °C, and from 600 °C to 900 °C. For instance, the percentages of weight loss after exposing the samples to 300 °C for about 1 h in a furnace were 3.15%, 2.87%, 2.68%, 2.61%, and 2.57%, at 0, 1, 2, 3, and 4% of NS dosages, respectively. These weight losses were increased to 6.54%, 6.13%, 5.97%, 5.77%, and 5.68% for the fire temperature of 600 °C. Further increments in weight loss were observed at a temperature of 900 °C, which was 10.6%, 10.19%, 9.93%, 9.61%, and 9.5% at 0, 1, 2, 3, and 4% of NS contents. On the other hand, it can be observed

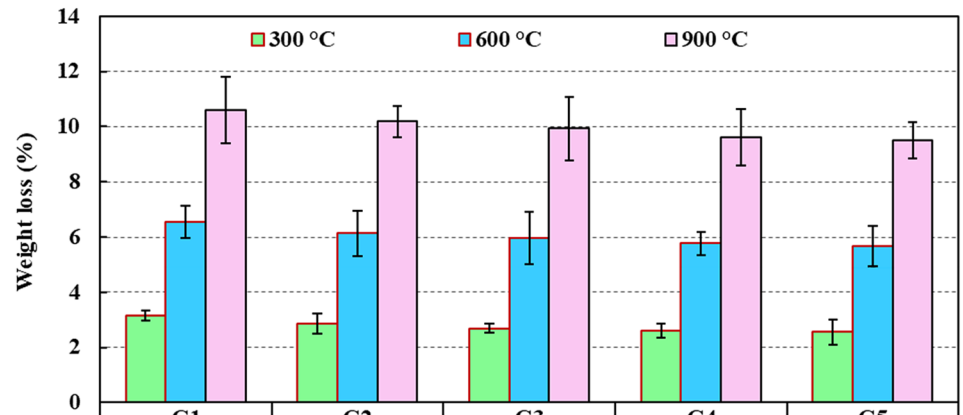

	G1	G2	G3	G4	G5
300 °C	3.15	2.87	2.68	2.61	2.57
600 °C	6.54	6.13	5.97	5.77	5.68
900 °C	10.60	10.19	9.93	9.61	9.50

Fig. 7 Weight loss of GPC mixtures with and without NS and RPA exposed to elevated temperatures

that adding NS to GGBFS-based geopolymer concrete lowered weight loss as NS dosages increased. For example, at 300 °C, the weight loss of geopolymer concrete specimens was improved by 8.76%, 14.75%, 17.05%, and 18.43%, at 1, 2, 3, and 4% NS content, respectively, compared to the control geopolymer concrete specimens without any dosages of NS. Additionally, it was found that the improvement in weight reduction caused by the presence of NS reduced as the temperature rose. For instance, the weight loss improvement at 600 °C was decreased to 6.21%, 8.65%, 11.75%, and 13.08%, and at 900 °C the weight loss improvement further decreased to 3.83%, 6.29%, 9.3%, and 10.4%, at 1, 2, 3, and 4% of NS inclusion, respectively. The evaporation of water from within the GPC constituents was found to be the cause of the weight losses of GPC specimens at lower elevated temperatures; however, at higher elevated temperatures, the mass loss was related to the breakdown of the internal components of the GPC specimens [47]. Furthermore, it was claimed that the reasons behind the deterioration of concrete composites due to fire damage were thermal dilatation and vapor pressure [48].

3.4.3 Residual Compressive Strength

To ensure that GPC can tolerate high temperatures, one aspect that has to be recognized is its thermal resistance. Figure 8 shows the residual compressive strength values measured for the control GPC sample and for GPC mixtures with different percentages of nano-silica. These results were obtained after the geopolymer concrete specimens were aged for 28 days and subjected to temperatures of 300 °C, 600 °C, and 900 °C. It was observed that as the temperature went from 300 °C to 600 °C, then from 600 °C to 900 °C, the compressive strength of the geopolymer concrete specimens significantly declined. On the other hand, it was found that the residual compressive strength improved as the doses of NS climbed. The residual compressive strength of geopolymer concrete mixtures decreased at a temperature of 300 °C by 6.71%, 5.21%, 4.40%, 3.62%, and 3.59%, at 0, 1, 2, 3, and 4% NS doses, respectively, when compared to its compressive strength in ambient curing conditions. Furthermore, when the fire temperature was raised to 600 °C, the residual compressive strength for the NS mentioned above loadings decreased by 18.46%, 15.64%, 14.08%, 13.09%, and 12.28%. In the same context, further decreases in compressive strength were seen at the temperature of 900 °C, which were 37.92%, 34.36%, 32.26%, 29.81%, and 27.84%, respectively, at 0, 1, 2, 3, and 4% of NS contents. As the heating temperature is extended, geopolymer concretes suffer more fire damage. Their strength gradually decreased when all samples were heated for 60 min. This could be explained by the matrix's growing shrinkage, which raises the thermal stresses around the aggregates and causes additional internal cracking [33].

These results indicated that the geopolymer concrete has a high resistance to elevated temperatures; this can be related to the microstructure of geopolymerization materials' pores. In addition, water is absent from the chemical makeup of geopolymerization materials. Compared to typical Portland cement concrete, hydrated cement requires water; as a result, calcium silicate hydrate C-S-H decomposes at high temperatures, resulting in a significant

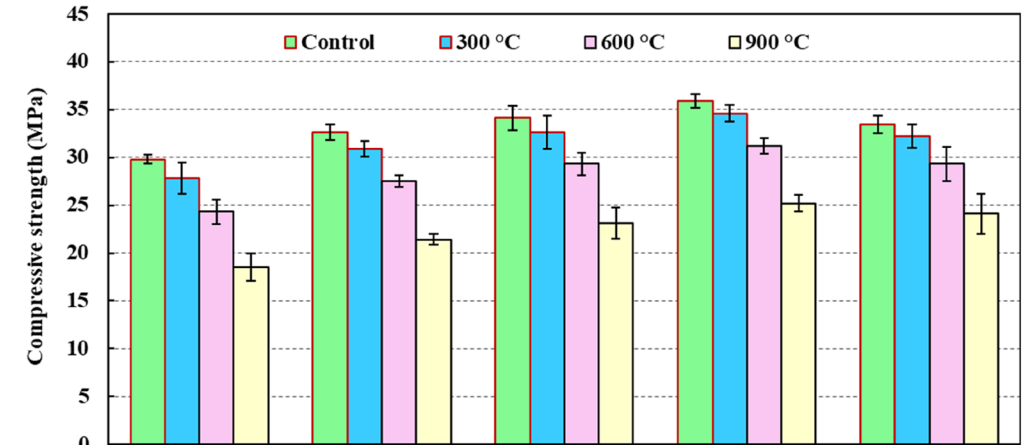

	G1	G2	G3	G4	G5
Control	29.8	32.6	34.1	35.9	33.4
300 °C	27.8	30.9	32.6	34.6	32.2
600 °C	24.3	27.5	29.3	31.2	29.3
900 °C	18.5	21.4	23.1	25.2	24.1

Fig. 8 Residual compressive strength of GPC mixtures with and without NS and RPA exposed to elevated temperatures

loss of mechanical strength [44]. On the other hand, Kong and Sanjayan [49] demonstrated that, when exposed to high temperatures, the geopolymer matrix can experience gradual shrinkage while the aggregates swell. This results in large cracks in the concrete composite, which is the primary cause of strength degradation [50]. Fire induces a temperature gradient, separating the cold core and hot surface layers and the tendency for the hot layer to flake off from the colder layer. The geopolymer matrix's disintegration resulted from several events during heating, including the evaporation of water that the N-A-S-H gel had absorbed, the production of water-free products, the melting, and the crystallization of stable water-free phases [51].

The filling impact of nanoparticles among the matrix's skeleton may be responsible for improving the resistance to elevated temperatures that result from the integration of sufficient NS content. According to reports, the filler caused an overall improvement in fire characteristics. Additionally, the heating procedure increased the reactivity of NS particles, which improved fire resistance [52]. By refereeing to the literature, similar results for improving the fire resistance of geopolymer composites have been observed, for instance, according to Estrada–Arreola et al. [53], adding NS using the sol–gel method to the alkaline solution for activated FA-based geopolymer pastes can increase their ability to resist fire. The specimens also demonstrated good micromechanical properties after being exposed to 1000 °C for two hours. Also, the impact of adding 0.5–3% NS to the blended fly ash/GGBFS-based geopolymer mortar was investigated by Revathi et al. [54]. The samples were heated to 200–800 °C for two hours. According to the findings, specimens with 0.5–2.5% NS after the fire had greater compressive strength retention than the control.

Furthermore, Fig. 9 depicts the compressive strength failure modes of G1 (control) and G4 (3%NS), after being exposed to elevated temperatures of 300 °C and 600 °C with and without varied NS dosages. After testing, several significant cracks on the concrete control specimens and those exposed to various NS doses point to a brittle failure mechanism. The failure mechanisms were shown to become more brittle as the temperature rose from 300 °C to 600 °C.

3.5 Electrical Conductivity

3.5.1 Bulk Electrical Conductivity

This test was conducted to determine the bulk electrical conductivity of saturated hardened concrete specimens according to ASTM C1760. This test method can be used as an easy assessment of durability indicators for service life prediction or quality control for concrete. It also provides a rapid indication of the concrete's resistance to the penetration of chloride ions by diffusion. Figure 10 depicts data on the bulk electrical conductivity of geopolymer concrete with and without various dosages of NS at 90 days. When the NS in the GPC mixtures increased, the value of bulk electrical conductivity decreased.

The bulk electrical conductivity of the control GPC specimen was 11.4 mS/m while adding NS at 1%, 2%, 3%, and 4% reduces the value of the GPC specimen's bulk electrical conductivity to 9.65, 8.95, 7.8, and 7.7 mS/m, respectively. Furthermore, the percentage improvements in bulk electrical conductivity values for the prior NS doses are 15.35%, 21.49%, 31.58%, and 32.46%, respectively, compared to the control GPC mixture without any NS dosages. This improvement was attributed to the fact that NS with a well-distributed and homogenous dispersion could significantly

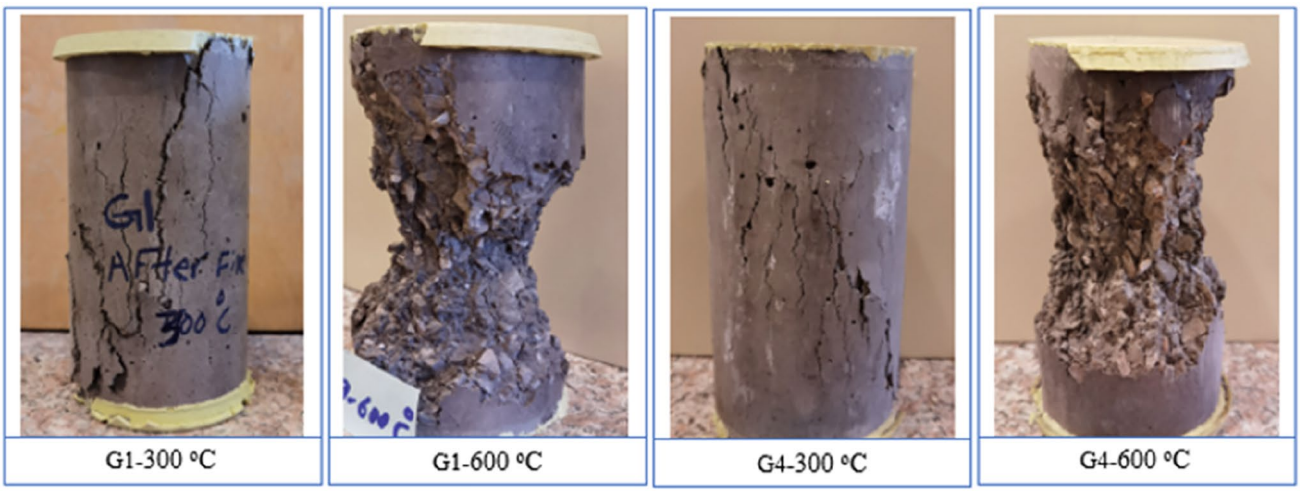

Fig. 9 GPC specimen failure patterns under compression test after being exposed to elevated temperatures of 300 °C and 600 °C

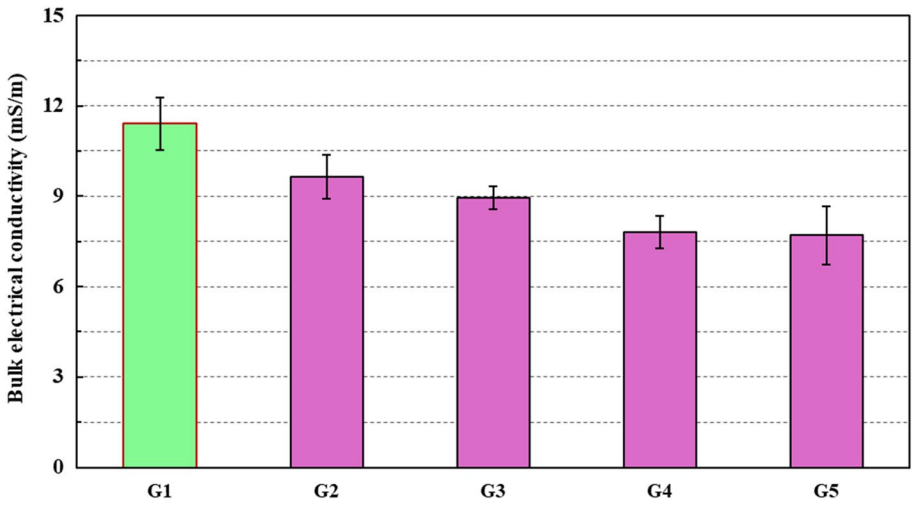

Fig. 10 Bulk electrical conductivity values of GPC mixtures with and without NS and RPA at the age of 90 days

improve particle packing in geopolymer concrete, resulting in a more compacted and denser microstructure, and as a consequence, chloride penetration was decreased and improved [10], moreover, lower bulk electrical conductivity value means that there are more crystalline compounds in nano-silica modified geopolymer concrete, the diffusion coefficient will be lower. This will make the material last longer and be more durable [55]. By referring to the literature, there is a huge gap regarding this test to evaluate the durability properties of geopolymer concrete modified with NS. Therefore, the authors of this study cannot compare their results with the previous works. Moreover, they believed these results could be helpful for scholars in the future, and researchers should use this test more to validate its results. Because adding NPs into the geopolymer concrete composites provides very fine particles to fill nanopores and voids as well as gives extra geopolymerization by products within the geopolymer system, improving the whole microstructure of the composite; on the other hand, adding NS improved the interfacial transition zones between the aggregates and matrix system. As a result, the inclusion of NS reduced the values of bulk electrical conductivity of all the geopolymer concrete mixtures in comparison to their reference mixes that did not contain any NS dosages.

3.5.2 Electrical Resistivity

Figure 11 shows the electrical resistivity test results of geopolymer concrete amended with various NS doses at 90 days. It was observed that the addition of NS raises the electrical resistivity values of all geopolymer concrete specimens. The electrical resistivity of the geopolymer concrete mixtures for the control specimens and different dosages of NS was in the range of 17.3 to 23.8 kΩ.cm. The inclusion of the NS to the GPC mixtures significantly improved the electrical resistivity of the specimens by 17.34%, 29.48%, 36.42%, and 37.28% at 1, 2, 3, and 4% NS dosages, respectively, compared to control geopolymer concrete specimens with

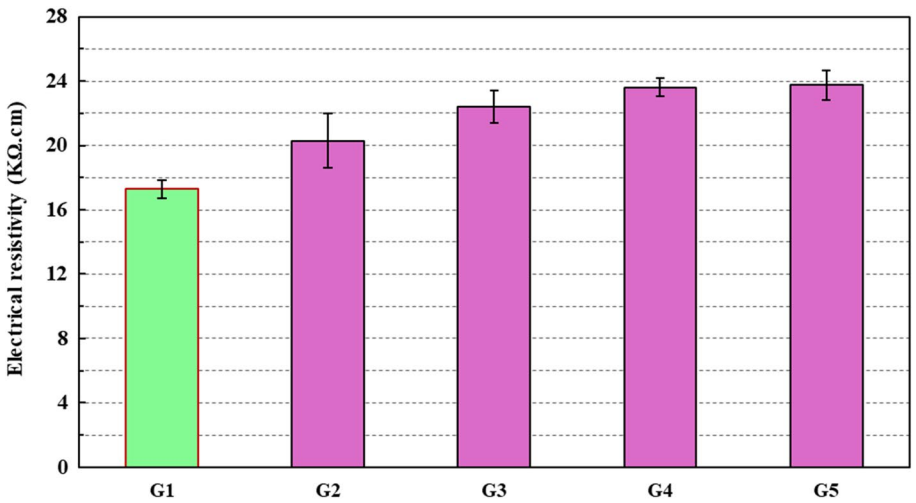

Fig. 11 Electrical resistivity values of GPC mixtures with and without NS and RPA at the age of 90 days

no dosages of NS. According to the guidelines of ACI 222R-01 [56], the test results showed that the rebar corrosion rate within these geopolymer concrete mixtures was moderate to low. It was also noted that adding NS to the geopolymer concrete mixtures changed the moderate corrosion rate to a low range, improving the performances of geoplymer concrete structures in harsh environmental conditions. It has been demonstrated that the electrical resistance of cementitious materials is directly influenced by the porosity and concentration of the ionized solution [57]. The specimens' resistance changes significantly when the doses of NS are increased. Adopting a greater monomer ratio decreases porosity and boosts resistance, delaying the entry of chlorine ions and enhancing durability. The ions will find it challenging to enter the specimen due to the increased electrical resistance, which will stop corrosion [58]. The addition of NS will produce extra C-S-H, N-A-S-H, and C-A-S-H gels and the filling nanopores in the geopolymer concrete matrixes [4]. Therefore, the matrix is compressed, and the free ion concentration is decreased, increasing the matrix's electrical resistance [59].

3.6 Multivariate Analysis

To save time, energy, and money, it is essential to develop a reliable and authoritative model for forecasting the various properties of geopolymer concrete. Modeling the properties of building materials can be done in various methods, including statistical methods, computer modeling, and more modern approaches like regression analysis and machine learning tools. Empirical regression analyses have been carried out to develop reliable empirical equations between mechanical and durability properties. Because the compressive strength of cement-based concrete composites, including geopolymer concretes, is the essential property, it was used to generate empirical equations. The simple correlations between compressive strength versus splitting tensile strength, flexural strength, modulus of elasticity, and electrical resistivity have been conducted to obtain the empirical equations. These equations were assessed by the coefficient of determination (R^2). In addition, the obtained results were compared to the same model codes like ACI 318, ACI 363, CEB-FIP, AS 3600, and EN, as well as some other developed empirical equations that are present in the literature studies.

3.6.1 Statistical Assessment for Experimental Results

In this section, to clarify the results of obtained experimental datasets, statistical functions such as Minimum, Maximum, Average, Standard Deviation, Skewness, Kurtosis, and Variance were calculated and displayed in Table 5 to show the distribution of each variable. Skewness is distortion or asymmetry in a symmetrical normal distribution in a dataset. If the curve is moved to the right or the left side, it is stated to be skewed. Also, skewness could be quantified as an impersonation of the range to which a given distribution differs from a normal distribution [60]. For instance, the skew of zero value was measured for normal distribution, while the right skew indicates the lognormal distribution. The kurtosis is a statistical indicator that explains how heavily the tails of a distribution of a set of data differ from the tails of the normal distribution. In addition, kurtosis finds the heaviness of the distribution tails, while skewness measures the symmetry of the distribution [61]. The variance is informed by the degree of spread in the dataset,the greater the spread of the data, the greater the variance is about the mean [14].

3.6.2 Correlations Between GPC Properties

3.6.2.1 Splitting Tensile Strength and Compressive Strength Multivariate analysis was conducted based on the laboratory experiment results to connect the splitting tensile strength results with the compressive strength, as shown in Fig. 12a. One can find a strong linear relationship between the compressive strength and the splitting tensile strength even though the concrete samples' age were 28 and 90 days. The outcomes of these relations are presented in Eqs. (1) and (2) for the curing ages of 28 and 90 days, respectively, with the coefficient of determinations (R^2) of 0.964 and 0.960. These Equations are valid for the GPC with a compressive strength greater than 30 MPa.

$$\mathbf{STS = 0.13\,CS - 0.57} \quad (1)$$

$$\mathbf{STS = 0.14\,CS - 1.06} \quad (2)$$

Table 5 Summary of statistical analysis of obtained experimental datasets

Test results	Min	Max	Average	SD	Variance	Skewness	Kurtosis
CS-28 days	29.8	35.9	33.16	2.24	5.01	− 0.62	1.19
CS-90 days	32.9	39.8	36.74	2.53	6.41	− 0.70	1.31
STS-28 days	3.31	4.08	3.74	0.30	0.09	− 0.64	− 0.17
STS-90 days	3.74	4.7	4.29	0.38	0.14	− 0.78	− 0.28
ER-90 days	17.3	23.75	21.47	2.71	7.34	− 1.09	0.18

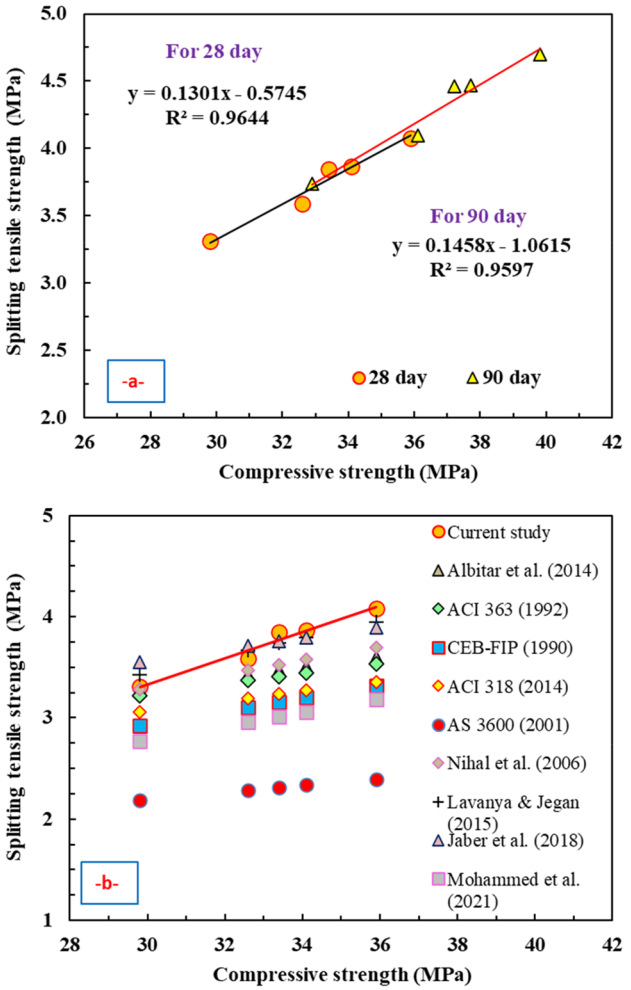

Fig.12 Correlation between splitting tensile strength and compressive strength, **a** Current study, **b** Comparison between literature and the current model

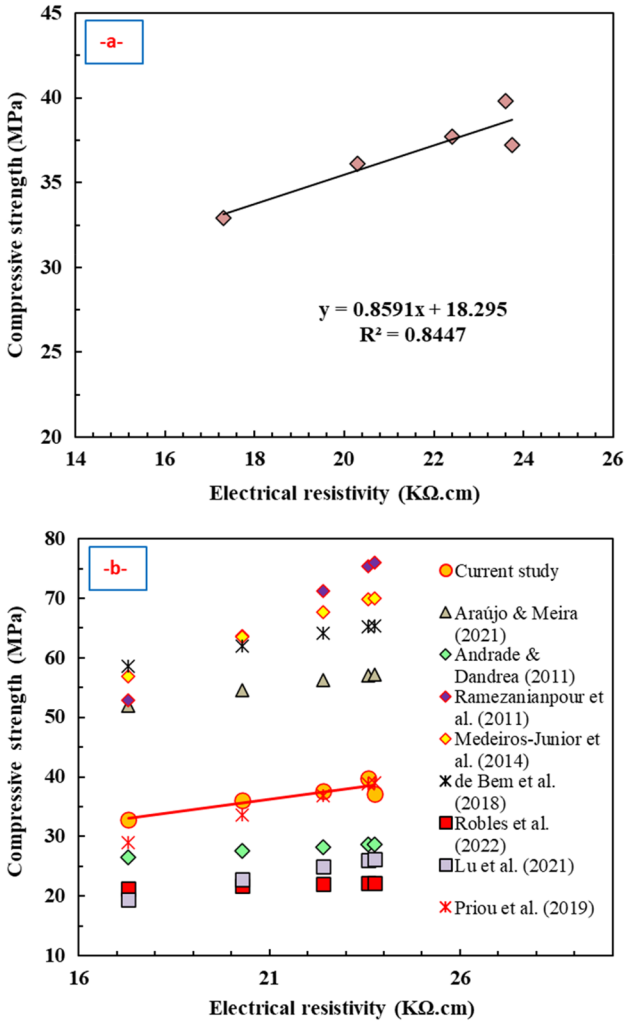

Fig. 13 Correlation between electrical resistivity and compressive strength **a** Current study, **b** Comparison between literature and the current model

where STS is the splitting tensile strength in MPa and CS is the compressive strength of the GPC specimens in MPa.

In addition, the created straightforward empirical equation for the age of 28 days was compared to various generated model codes and other developed empirical equations found in the literature, as depicted in Fig. 12b. It was discovered that adopting the equations proposed by AS 3600 [62] and CEB-FIP [63] for predicting the splitting tensile strength of GPC incorporating varying dosages of NS has no possibility of success because it drastically underestimates the test data. Similarly, empirical models suggested by Mohammed et al. [8] underestimate the test results. However, this equation was derived from 598 datasets from 54 past studies. Also, the equations given by ACI 318 [64], ACI 363 [65], Nihal et al. [66] and Albitar et al. [67] are nearly the same. They well matched with the test data for GPC of compressive strength lower than about 30 MPa and underestimated the results of the tested specimens for the concrete compressive strength greater than 30 MPa. However, the model equations proposed bt Lavanya & Jegan [68] and Jaber et al. [69] are well-matched with the tested experimental results.

3.6.2.2 Electrical Resistivity and Compressive Strength As previously stated, electrical resistivity is a nondestructive test for evaluating the properties of concrete composites, so forecasting the compressive strength of GPC using this test technique will be interesting. Based on the obtained experimental laboratory results, a simple regression analysis has been conducted to correlate the results of the electrical resistivity with the compressive strength, as depicted in Fig. 13a. The compressive strength and electrical resistivity of GPC mixtures were shown to be strongly correlated linearly. The results of these relations for curing ages of 90 days are provided by Eq. (3), which has coefficients of determination

(R^2) of 0.845. These equations are valid for the GPC with an electrical resistivity greater than 17 KΩ.cm.

$$\mathbf{CS = 0.859\,ER + 18.3} \quad (3)$$

where CS is the compressive strength in MPa and ER is the electrical resistivity of the GPC specimens in (KΩ.cm). This developed equation was compared to other generated model codes and other developed empirical equations found in the literature, much like the sub-sections above, as illustrated in Fig. 13b.

The equations proposed by Ramezanianpour et al. [70], Medeiros-Junior et al. [71], de Bem et al. [72], and Araujo & Meira [73] were found to significantly overestimate the test data, making it impossible to predict the compressive strength of GPC incorporated different dosages of NS based on their electrical resistivity results. In the same context, model equations by Andrade and Dandrea [74], Lu et al. [75], and Robles et al. [76] were not advised for predicting the compressive strength of GPC from their electrical resistivity test results because, in contrast to the previous equations, they underestimated the test data of GPC incorporating different dosages of NS. On the other hand, it was found that the predictions of Priou et al. [77] are regarded as safe and accurate for forecasting the compressive strength of GPC from their experimental electrical resistivity of greater then 20 KΩ.cm, otherwise underestimated the results. Finally, it was found that none of the model or suggested empirical equations in the literature correspond to the experimental results. This is because the situation of these GPC mixtures differs greatly from that of standard and other types of concretes due to the nature of geopolymer system as well as its curing conditions.

3.7 Microstructural Properties

3.7.1 Scanning Electron Microscope (SEM)

As previously mentioned, the main method of enhancing the characteristics of geopolymer using various nanomaterials is through enhancing its microstructure. Figures 14a through h illustrate the microstructure of GPC specimens (G1) and GPC mixtures containing 3% of NS at different scales ranging from 2 µm to 200 nm. These figures clearly showed that the addition of NS improved and enhanced the microstructure of the GPC mixtures. Figures 14a, c, e, and g show the microstructure of the control GPC specimens without any NS dosages; these figures illustrated that the morphological growth of the GPC mixtures lacking NS is extremely porous and heterogeneous in the ambient curing conditions. However, incorporating NS leads to the product's microstructure becoming uniform and more compact, as can be seen in Fig. 14b, d, f, and h. These findings highlight how the mechanical and durability characteristics of GPC mixtures with NS addition have improved compared to control GPC specimens because the greater strength properties are typically seen in geopolymer materials with decreased porosity, increased density, and a condensed microstructure [78]. On the other hand, Si, Al, and alkali activators' chemical interactions influenced the enhancement of GC's microstructure,the addition of NS will strengthen the Si components and speed up the stimulation of the geopolymer in the GC mixture [15]. The use of nanomaterials in the polymerization process and nanofiller capacity considerably improves the bonding interface and material permeability. Microscopic inspection is often used to analyze the evolution of geopolymer microstructure. Microscopic inspection is often used to analyze the evolution of microstructure in geopolymers. The density and porosity of the structure are directly proportional to the mechanical and durability performance of the composites, which are also influenced by the GC's shape [79].

Similar findings in enhancing the microstructure of various source binder materials based-GPC have been discovered by reviewing the literature. For instance, Khater [80] was found that the morphological growth of the GGBFS geopolymer lacking NS is extremely porous and heterogeneous. Deb et al. [81] reported a similar conclusion: adding 2% NS to GGBFS-based FA geopolymer resulted in a harder and more compact morphology. Moreover, according to a research finding by Mustakim et al. [16], unreacted silica particles become activated over time, making the product's microstructure compact and uniform. Furthermore, Behfarnia and Rostami [15] examined the microstructure of GGBFS-based GPC with micro and NS. Because of the pozzolanic activity of NS, which gradually occupies the Nano gaps, the creation of additional polymer gels triggered the discovery of NS included in the geopolymer mixture. This gel clings to particles, filling gaps and connecting them. Similarly, Ibrahim et al. [82] demonstrated how adding NS altered geopolymer concrete's mechanical characteristics and morphology.

3.7.2 Thermogravimetric Analysis (TGA)

The thermal stability of the geopolymer concrete specimens was evaluated in this work using thermogravimetry analysis (TGA). TGA is an effective method for assessing the thermal stability of materials, especially polymers. This method shows differences in a specimen's weight as its temperature rises [10]. The TGA test was performed for control and optimum nano dosage samples at 28 days. The output of the TGA test results is presented in Fig. 15. In general, it is evident that after being subjected to TGA thermal analysis up to 600 °C, the weight of both GPC specimens decreases. It was demonstrated that weight loss increased as the TGA device's tem-

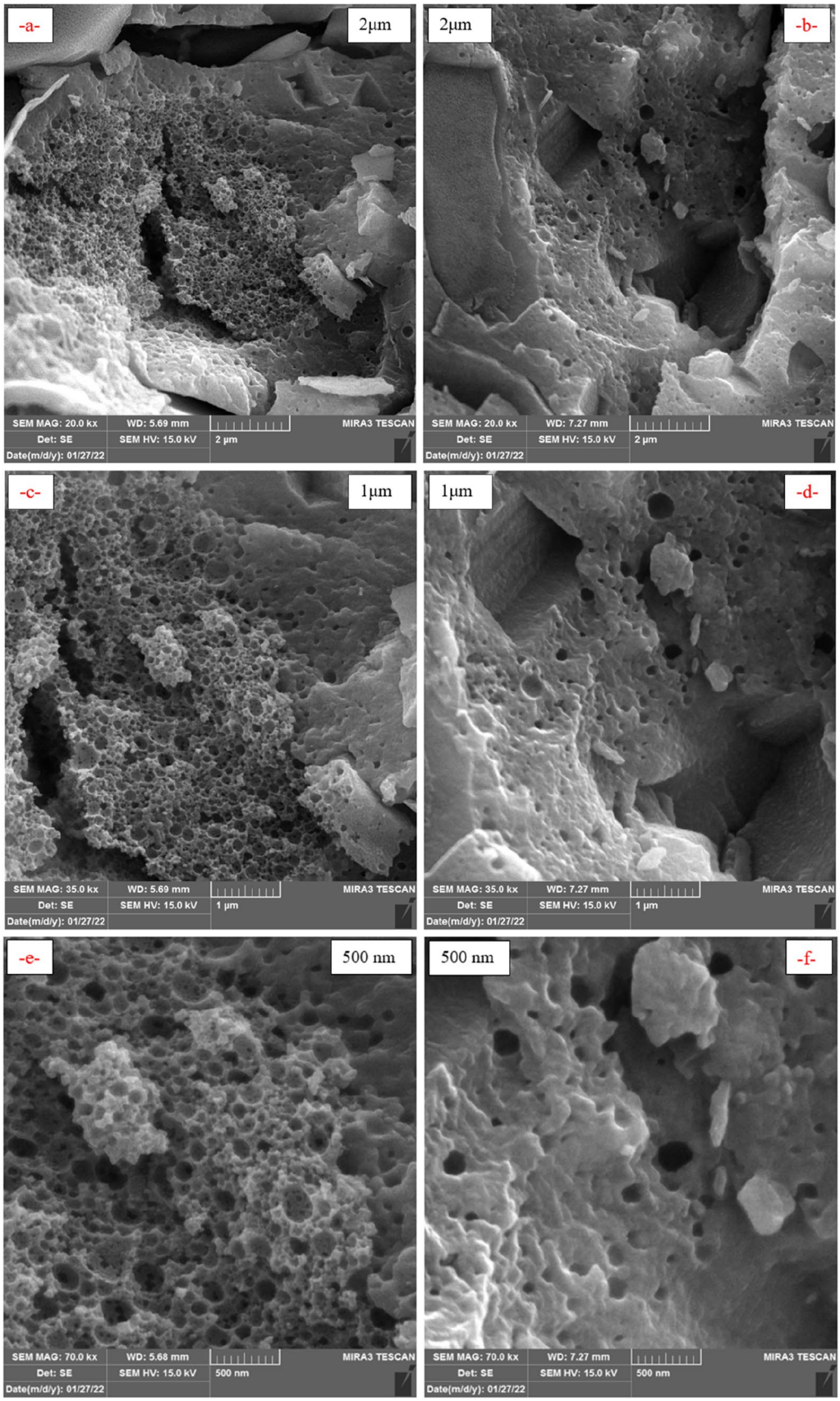

Fig. 14 SEM image of **a, c, e,** and **g** GPC specimen without NS; **b, d, f,** and **h** GPC specimen with 3% NS

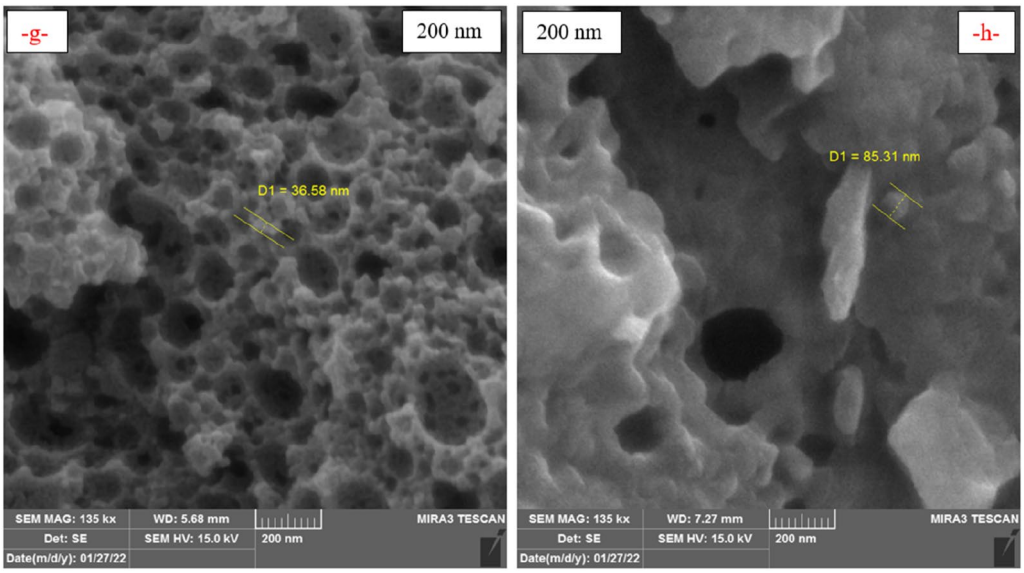

Fig. 14 (continued)

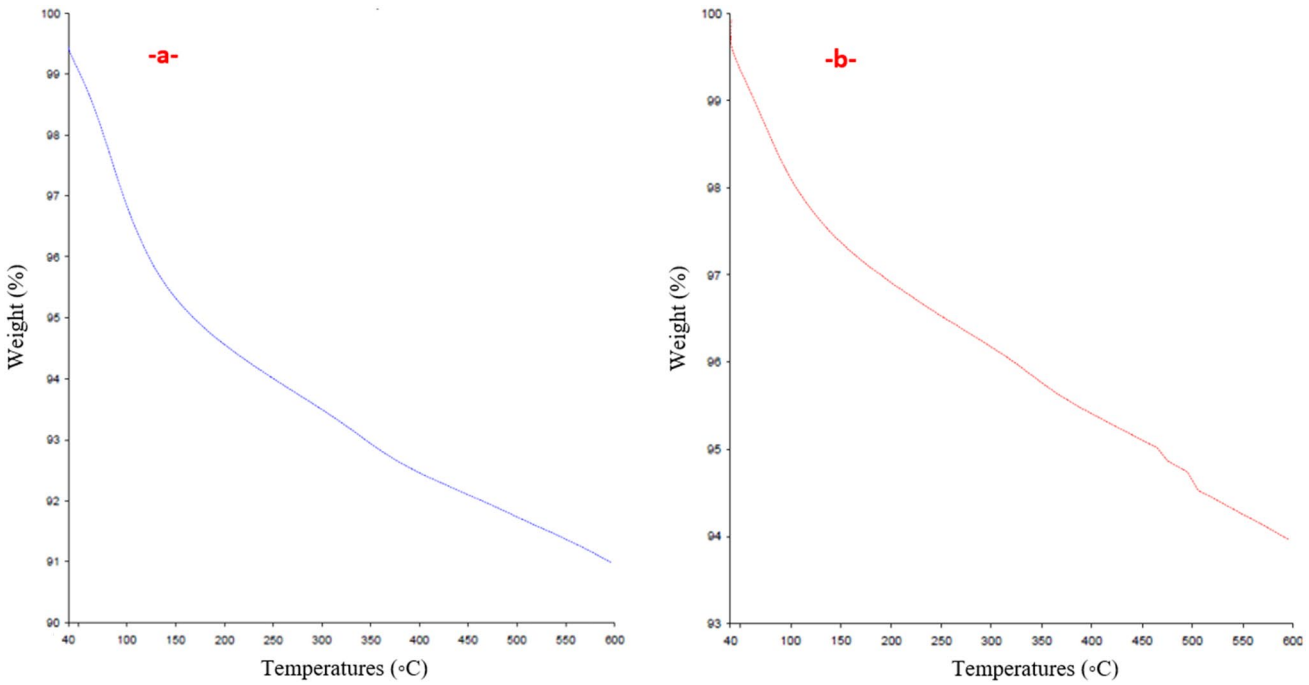

Fig. 15 TGA thermal analysis of GPC mixtures **a** Without NS, **b**: With 3% NS

perature rose for specimens made of control and nano-geopolymer concrete. Moreover, both GPC samples experienced greater weight loss up to 180 °C, moderately increasing to 600 °C. This is because the free water is evaporated up to 125 C, while the gradual weight loss up to 350 °C is happened due to the evaporation of structural or combined water. However, the weight loss of GPC specimens after 350 C was caused by the de-hydroxylation of the chemically bound silicon-hydroxyl group, which yields silicon-oxygen group and evaporated water [83–85].

On the other hand, as shown in Fig. 15, the geopolymer concrete with 3% NS (Fig. 15a) performed better in terms of weight loss (6% vs. 9%) than the control specimens with no NS doses (Fig. 15b). These outcomes were attributable to NS's inclusion, which generated extra C-S-H gels with high temperature resistance [27, 28]. By consulting the

literature, it was discovered that several other researchers had found results that were comparable to those of this study. For instance, Revathi et al. [54] conducted an experimental study to demonstrate the impact of adding NS on the microstructure and thermo-mechanical properties of blended fly ash/GGBFS-based geopolymer mortar composites. They discovered that the geopolymer mortar containing NS performed better in weight reduction than the control specimens with no NS doses. Moreover, the effects of adding nano-clay (NC) on the microstructural, thermal, and mechanical properties of flax fabric-reinforced geopolymer paste composites were examined by Assaedi et al. [86, 87]. The weight loss of the geopolymer paste decreased at dosages of 1.0, 2.0, and 3.0% of NC from 12.4 to 12.1 and 11.5–11.8%, respectively. This showed that the largest improvement in the geopolymer matrix's heat stability occurred at 2.0% of NC loading.

4 Conclusions

The following conclusions were reached after conducting extensive laboratory experiments on the setting times, mechanical, fire resistance, and microstructural properties of geopolymer concrete incorporating different dosages of nano-silica:

1. The initial and final setting times of geopolymer paste mixtures were increased with increasing the dosages of NS to the geopolymer paste mixtures. The maximum initial and final setting time occurred at 4% of NS doses of 47 and 37%, respectively, relative to the control geopolymer paste mixtures.
2. The compressive strength of the geopolymer concrete mixtures increased with increasing NS dosages up to 3%, and then it declined. Moreover, when the sample ages grew, the compressive strength values also grew. The largest improvement in compressive strength occurred at 3% NS, which was 6.3, 13.4, 20.5, 21, and 21.9% at curing ages of 3, 7, 28, 90, and 180 days.
3. The effect of incorporating NS into geopolymer concrete mixtures on the splitting tensile strength of all geopolymer concrete mixtures was similar to that of compressive strength, except that 2% NS was the optimum dosage for providing maximum flexural strength.
4. The maximum improvement in the splitting tensile strength of geopolymer concrete mixtures was 23.3 and 25.7% at 28 and 90 days.
5. The electrical resistivity and bulk electrical conductivity of geopolymer concrete was significantly improved as different dosages of nano-silica were added to the GPC mixtures. The maximum improvement in the electrical resistivity and bulk electrical conductivity was nearly similar for NS dosages of 3 and 4%, which were about 36.7 and 32%, respectively, at the age of 90 days, compared to the control GPC specimens.
6. Adding NS to geopolymer concrete specimens increased their resilience to moderate and high elevated temperatures in terms of visual appearance, weight loss, and residual compressive strength. Also, based on the TGA analysis, the weight loss of geopolymer concrete specimens modified with NS was lower than those geopolymer concrete specimens without any dosages of NS.
7. After exposure to the elevated temperatures, the weight loss of GPC specimens decreased as the content of NS rose in the GPC mixtures. The maximum improvement in the weight loss was recorded for 4% of NS, which is very close to that GPC mixture that contains 3% NS, and it was 18.4, 13.1, and 10.4% lower than the control GPC mixture at the elevated temperatures of 300 °C, 600 °C, and 900 °C, respectively.
8. Afetr exposure to the elevated temperatures, the residual compressive strength of the control geopolymer concrete mixture was 6.7, 18.5, and 38% lower than its compressive strength at ambient curing conditions for the elevated temperatures of 300 °C, 600 °C, and 900 °C, respectively. However, these values decreased nearly to 3.6, 12.5, and 28% for GPC mixtures incorporated both 3 and 4% of NS for the previously elevated temperatures.
9. According to the SEM images, adding NS to geopolymer concrete mixtures improved the matrix and the interfacial transition zones between aggregates and the geopolymer matrix. Consequently, improved other mechanical and durability properties.
10. It is not suitable to predict the splitting tensile strength from tested compressive strength values using the model codes and empirical equations that have been developed and presented in the literature. Also, it is unsuitable to predict the compressive strength of GPC specimens using model codes or other proposed empirical equation based on its electrical resistivity results.

Author contributions Ahmed Salih, Hemn: Conceptualization, Methodology, Modeling Azad: Data curation, Writing- Original draft preparation. Hemn: Visualization, Investigation. Ahmed and Hemn: Supervision.: Ahmed: Validation.: Hemn: Writing- Reviewing and Editing,

Funding Not applicable.

Data Availability All data generated or analyzed during this study are included in this published article.

Declarations

Conflict of interest We wish to confirm that there are no known conflicts of interest associated with this publication, and there has been no significant financial support for this work that could have influenced its outcome.

Research involving human and animal participants This article does not contain any studies involving animals performed by any of the authors. This article does not contain any studies involving human participants performed by any of the authors.

References

1. G. Habert, S.A. Miller, V.M. John, J.L. Provis, A. Favier, A. Horvath, K.L. Scrivener, Environmental impacts and decarbonization strategies in the cement and concrete industries. Nat. Rev. Earth Environ. **1**(11), 559–573 (2020). https://doi.org/10.1038/s43017-020-0093-3
2. E. Gartner, Industrially interesting approaches to "low-CO2" cements. Cem. Concr. Res. **34**(9), 1489–1498 (2004). https://doi.org/10.1016/j.cemconres.2004.01.021
3. X. Guo, H. Shi, W.A. Dick, Compressive strength and microstructural characteristics of class C fly ash geopolymer. Cement Concr. Compos. **32**(2), 142–147 (2010). https://doi.org/10.1016/j.cemconcomp.2009.11.003
4. H.U. Ahmed, A.A. Mohammed, A.S. Mohammad, The role of nanomaterials in geopolymer concrete composites: a state-of-the-art review. J. Build. Eng. (2022). https://doi.org/10.1016/j.jobe.2022.104062
5. J.L. Provis, S.A. Bernal, Geopolymers and related alkali-activated materials. Annu. Rev. Mater. Res. **44**, 299–327 (2014). https://doi.org/10.1146/annurev-matsci-070813-113515
6. J. Davidovits, *Polymers and geopolymers. Geopolymer Chemistry and Applications*, 4th edn. (Institut Géopolymère, Saint Quentin, 2015)
7. H.U. Ahmed, A.A. Mohammed, S. Rafiq, A.S. Mohammed, A. Mosavi, N.H. Sor, S. Qaidi, Compressive strength of sustainable geopolymer concrete composites: a state-of-the-art review. Sustainability **13**(24), 13502 (2021). https://doi.org/10.3390/su132413502
8. A.A. Mohammed, H.U. Ahmed, A. Mosavi, survey of mechanical properties of geopolymer concrete: a comprehensive review and data analysis. Materials **14**(16), 4690 (2021). https://doi.org/10.3390/ma14164690
9. A. Hassan, M. Arif, M. Shariq, Effect of curing condition on the mechanical properties of fly ash-based geopolymer concrete. SN Appl. Sci. **1**(12), 1–9 (2019). https://doi.org/10.1007/s42452-019-1774-8
10. H.U. Ahmed, A.A. Mohammed, A. Mohammed, Soft computing models to predict the compressive strength of GGBS/FA-geopolymer concrete. PLoS ONE **17**(5), e0265846 (2022). https://doi.org/10.1371/journal.pone.0265846
11. H.H. Sharif, Fresh and mechanical characteristics of eco-efficient geopolymer concrete incorporating nano-silica: an overview. Kurdistan J. Appl. Res. (2021). https://doi.org/10.24017/science.2021.2.6
12. A. Lazaro, Q.L. Yu, H.J.H. Brouwers, Nanotechnologies for sustainable construction, in *Sustainability of construction materials*. (Woodhead Publishing, Sawston, 2016), pp.55–78
13. B.B. Jindal, R. Sharma, The effect of nanomaterials on properties of geopolymers derived from industrial by-products: a state-of-the-art review. Constr. Build. Mater. **252**, 119028 (2020)
14. R.H. Faraj, H.U. Ahmed, S. Rafiq, N.H. Sor, D.F. Ibrahim, S.M. Qaidi, Performance of self-compacting mortars modified with nanoparticles: a systematic review and modeling. Cleaner Mater. (2022). https://doi.org/10.1016/j.clema.2022.100086
15. K. Behfarnia, M. Rostami, Effects of micro and nanoparticles of SiO2 on the permeability of alkali activated slag concrete. Constr. Build. Mater. **131**, 205–213 (2017). https://doi.org/10.1016/j.conbuildmat.2016.11.070
16. S.M. Mustakim, S.K. Das, J. Mishra, A. Aftab, T.S. Alomayri, H.S. Assaedi, C.R. Kaze, Improvement in fresh, mechanical and microstructural properties of fly ash-blast furnace slag based geopolymer concrete by addition of nano and micro silica. SILICON **13**(8), 2415–2428 (2021). https://doi.org/10.1007/s12633-020-00593-0
17. A. Çevik, R. Alzeebaree, G. Humur, A. Niş, M.E. Gülşan, Effect of nano-silica on the chemical durability and mechanical performance of fly ash based geopolymer concrete. Ceram. Int. **44**(11), 12253–12264 (2018). https://doi.org/10.1016/j.ceramint.2018.04.009
18. M.A. Kotop, M.S. El-Feky, Y.R. Alharbi, A.A. Abadel, A.S. Binyahya, Engineering properties of geopolymer concrete incorporating hybrid nano-materials. Ain Shams Eng. J. **12**(4), 3641–3647 (2021). https://doi.org/10.1016/j.asej.2021.04.022
19. G. Saini, U. Vattipalli, Assessing properties of alkali activated GGBS based self-compacting geopolymer concrete using nano-silica. Case Stud. Constr. Mater. **12**, e00352 (2020). https://doi.org/10.1016/j.cscm.2020.e00352
20. F. Shahrajabian, K. Behfarnia, The effects of nano particles on freeze and thaw resistance of alkali-activated slag concrete. Constr. Build. Mater. **176**, 172–178 (2018). https://doi.org/10.1016/j.conbuildmat.2018.05.033
21. R. Alzeebaree, Bond strength and fracture toughness of alkali activated self-compacting concrete incorporating metakaolin or nanosilica. Sustainability **14**(11), 6798 (2022). https://doi.org/10.3390/su14116798
22. A. Mohammedameen, Performance of alkali-activated self-compacting concrete with incorporation of nanosilica and metakaolin. Sustainability **14**(11), 6572 (2022). https://doi.org/10.3390/su14116572
23. H.U. Ahmed, A.S. Mohammed, R.H. Faraj, S.M. Qaidi, A.A. Mohammed, Compressive strength of geopolymer concrete modified with nano-silica: experimental and modeling investigations. Case Stud. Constr. Mater. (2022). https://doi.org/10.1016/j.cscm.2022.e01036
24. M.S Reddy, P. Dinakar, & B.H. Rao, Mix design development of fly ash and ground granulated blast furnace slag based geopolymer concrete. J. Build. Eng. **20**, 712–722 (2018)
25. N. Li, C. Shi, Z. Zhang, H. Wang, & Y. Liu, A review on mixture design methods for geopolymer concrete. Compos. B. Eng. **178**, 107490 (2019)
26. P. Chindaprasirt, U. Rattanasak, S. Taebuanhuad, Resistance to acid and sulfate solutions of microwave-assisted high calcium fly ash geopolymer. Mater. Struct. **46**(3), 375–381 (2013). https://doi.org/10.1617/s11527-012-9907-1
27. G.F. Huseien, H.K. Hamzah, A.R.M. Sam, N.H.A. Khalid, K.W. Shah, D.P. Deogrescu, J. Mirza, Alkali-activated mortars blended with glass bottle waste nano powder: Environmental benefit and sustainability. J. Clean. Prod. **243**, 118636 (2020). https://doi.org/10.1016/j.jclepro.2019.118636
28. M. Samadi, K.W. Shah, G.F. Huseien, N.H.A.S. Lim, Influence of glass silica waste nano powder on the mechanical and microstructure properties of alkali-activated mortars. Nanomaterials **10**(2), 324 (2020). https://doi.org/10.3390/nano10020324

29. X. Gao, Q.L. Yu, H.J.H. Brouwers, Characterization of alkali activated slag–fly ash blends containing nano-silica. Constr. Build. Mater. **98**, 397–406 (2015). https://doi.org/10.1016/j.conbuildmat.2015.08.086
30. T. Phoo-ngernkham, P. Chindaprasirt, V. Sata, S. Hanjitsuwan, S. Hatanaka, The effect of adding nano-SiO2 and nano-Al2O3 on properties of high calcium fly ash geopolymer cured at ambient temperature. Mater. Des. **55**, 58–65 (2014). https://doi.org/10.1016/j.matdes.2013.09.049
31. U. Durak, O. Karahan, B. Uzal, S. İlkentapar, C.D. Atiş, Influence of nano SiO2 and nano CaCO3 particles on strength, workability, and microstructural properties of fly ash-based geopolymer. Struct. Concr. **22**, E352–E367 (2021). https://doi.org/10.1002/suco.201900479
32. M. Etemadi, M. Pouraghajan, H. Gharavi, Investigating the effect of rubber powder and nano silica on the durability and strength characteristics of geopolymeric concretes. J. Civil Eng. Mater. Appl. **4**(4), 243–252 (2020). https://doi.org/10.22034/jcema.2020.119979
33. P. Nuaklong, P. Jongvivatsakul, T. Pothisiri, V. Sata, P. Chindaprasirt, Influence of rice husk ash on mechanical properties and fire resistance of recycled aggregate high-calcium fly ash geopolymer concrete. J. Clean. Prod. **252**, 119797 (2020). https://doi.org/10.1016/j.jclepro.2019.119797
34. A.A. Ramezanianpour, M.A. Moeini, Mechanical and durability properties of alkali activated slag coating mortars containing nanosilica and silica fume. Constr. Build. Mater. **163**, 611–621 (2018). https://doi.org/10.1016/j.conbuildmat.2017.12.062
35. K. Sun, X. Peng, S. Wang, L. Zeng, P. Ran, G. Ji, Effect of nano-SiO2 on the efflorescence of an alkali-activated metakaolin mortar. Constr. Build. Mater. **253**, 118952 (2020). https://doi.org/10.1016/j.conbuildmat.2020.118952
36. J.M. Their, M. Özakça, Developing geopolymer concrete by using cold-bonded fly ash aggregate, nano-silica, and steel fiber. Constr. Build. Mater. **180**, 12–22 (2018). https://doi.org/10.1016/j.conbuildmat.2018.05.274
37. S. Naskar, A.K. Chakraborty, Effect of nano materials in geopolymer concrete. Perspect. Sci. **8**, 273–275 (2016). https://doi.org/10.1016/j.pisc.2016.04.049
38. P. Zhang, K. Wang, J. Wang, J. Guo, S. Hu, Y. Ling, Mechanical properties and prediction of fracture parameters of geopolymer/alkali-activated mortar modified with PVA fiber and nano-SiO2. Ceram. Int. **46**(12), 20027–20037 (2020). https://doi.org/10.1016/j.ceramint.2020.05.074
39. N. Hamed, M.S. El-Feky, M. Kohail, E.S.A. Nasr, Effect of nano-clay de-agglomeration on mechanical properties of concrete. Constr. Build. Mater. **205**, 245–256 (2019). https://doi.org/10.1016/j.conbuildmat.2019.02.018
40. B. Mahboubi, Z. Guo, H. Wu, Evaluation of durability behavior of geopolymer concrete containing nano-silica and nano-clay additives in acidic media. J. Civil Eng. Mater. Appl. **3**(3), 163–171 (2019). https://doi.org/10.22034/JCEMA.2019.95839
41. E. Rabiaa, R.A.S. Mohamed, W.H. Sofi, T.A. Tawfik, Developing geopolymer concrete properties by using nanomaterials and steel fibers. Adv. Mater. Sci. Eng. (2020). https://doi.org/10.1155/2020/5186091
42. D. Adak, M. Sarkar, S. Mandal, Structural performance of nano-silica modified fly-ash based geopolymer concrete. Constr. Build. Mater. **135**, 430–439 (2017). https://doi.org/10.1016/j.conbuildmat.2016.12.111
43. S. Vyas, S. Mohammad, S. Pal, N. Singh, Strength and durability performance of fly ash based geopolymer concrete using nano silica. Int. J. Eng. Sci. Technol. **4**(2), 1–12 (2020). https://doi.org/10.29121/ijoest.v4.i2.2020.73
44. A. Nazari, A. Bagheri, J.G. Sanjayan, M. Dao, C. Mallawa, P. Zannis, S. Zumbo, Thermal shock reactions of ordinary portland cement and geopolymer concrete: microstructural and mechanical investigation. Constr. Build. Mater. **196**, 492–498 (2019). https://doi.org/10.1016/j.conbuildmat.2018.11.098
45. A. Fernández-Jiménez, J.Y. Pastor, A. Martín, A. Palomo, High-temperature resistance in alkali-activated cement. J. Am. Ceram. Soc. **93**(10), 3411–3417 (2010). https://doi.org/10.1111/j.1551-2916.2010.03887.x
46. W.D. Rickard, C.S. Kealley, A. Van Riessen, Thermally induced microstructural changes in fly ash geopolymers: experimental results and proposed model. J. Am. Ceram. Soc. **98**(3), 929–939 (2015). https://doi.org/10.1111/jace.13370
47. J. Zhao, K. Wang, S. Wang, Z. Wang, Z. Yang, E.D. Shumuye, X. Gong, Effect of elevated temperature on mechanical properties of high-volume fly ash-based geopolymer concrete, mortar and paste cured at room temperature. Polymers **13**(9), 1473 (2021). https://doi.org/10.3390/polym13091473
48. M. Ozawa, S. Uchida, T. Kamada, H. Morimoto, Study of mechanisms of explosive spalling in high-strength concrete at high temperatures using acoustic emission. Constr. Build. Mater. **37**, 621–628 (2012). https://doi.org/10.1016/j.conbuildmat.2012.06.070
49. D.L. Kong, J.G. Sanjayan, Damage behavior of geopolymer composites exposed to elevated temperatures. Cement Concr. Compos. **30**(10), 986–991 (2008). https://doi.org/10.1016/j.cemconcomp.2008.08.001
50. D.L. Kong, J.G. Sanjayan, K. Sagoe-Crentsil, Comparative performance of geopolymers made with metakaolin and fly ash after exposure to elevated temperatures. Cem. Concr. Res. **37**(12), 1583–1589 (2007). https://doi.org/10.1016/j.cemconres.2007.08.021
51. F. Farooq, X. Jin, M.F. Javed, A. Akbar, M.I. Shah, F. Aslam, R. Alyousef, Geopolymer concrete as sustainable material: a state of the art review. Constr. Build. Mater. **306**, 124762 (2021)
52. A.M. Rashad, A.S. Ouda, Thermal resistance of alkali-activated metakaolin pastes containing nano-silica particles. J. Therm. Anal. Calorim. **136**(2), 609–620 (2019). https://doi.org/10.1007/s10973-018-7657-1
53. F. Estrada-Arreola, J.J. Pérez-Bueno, F.J. Flores-Ruíz, E. León-Sarabia, F.J. Espinoza-Beltrán The effect of temperature on micro-mechanical properties of fly ash based geopolymers activated with nano-SiO2 solution by sol-gel technique. Microscopy: Adv. Sci. Res. Educ. 986–991 (2014)
54. T. Revathi, R. Jeyalakshmi, N.P. Rajamane, Study on the role of n-SiO2 incorporation in thermo-mechanical and microstructural properties of ambient cured FA-GGBS geopolymer matrix. Appl. Surf. Sci. **449**, 322–331 (2018). https://doi.org/10.1016/j.apsusc.2018.01.281
55. D. Adak, M. Sarkar, S. Mandal, Effect of nano-silica on strength and durability of fly ash based geopolymer mortar. Constr. Build. Mater. **70**, 453–459 (2014). https://doi.org/10.1016/j.conbuildmat.2014.07.093
56. ACI Committee 222, Protection of metals in concrete against corrosion, ACI 222R-01, 2001.
57. E. Mohseni, B.M. Miyandehi, J. Yang, M.A. Yazdi, Single and combined effects of nano-SiO2, nano-Al2O3 and nano-TiO2 on the mechanical, rheological and durability properties of self-compacting mortar containing fly ash. Constr. Build. Mater. **84**, 331–340 (2015). https://doi.org/10.1016/j.conbuildmat.2015.03.006
58. E. Mohseni, Assessment of Na2SiO3 to NaOH ratio impact on the performance of polypropylene fiber-reinforced geopolymer composites. Constr. Build. Mater. **186**, 904–911 (2018). https://doi.org/10.1016/j.conbuildmat.2018.08.032
59. A.A. Ramezanianpour, F. Bahman Zadeh, A. Zolfagharnasab, A.M. Ramezanianpour, Mechanical properties and chloride ion penetration of alkali activated slag concrete, in *High tech*

concrete: where technology and engineering meet. (Springer, Cham, 2018), pp.2203–2212. https://doi.org/10.1007/978-3-319-59471-2_252
60. H.U. Ahmed, A.S. Mohammed, A.A. Mohammed, R.H. Faraj, Systematic multiscale models to predict the compressive strength of fly ash-based geopolymer concrete at various mixture proportions and curing regimes. PLoS ONE **16**(6), e0253006 (2021). https://doi.org/10.1371/journal.pone.0253006
61. H.U. Ahmed, A.S. Mohammed, S.M.A. Qaidi, R.H. Faraj, N.H. Sor, A.A. Mohammed, Compressive strength of geopolymer concrete composites: a systematic comprehensive review, analysis and modeling. Eur. J. Environ. Civ. Eng. (2022). https://doi.org/10.1080/19648189.2022.2083022
62. AS, A. S. 2001. Concrete structures. *AS3600–2001. Sydney (Australia): Standards Australia*.
63. Committee Euro-International du Beton (CEB-FIP). CEB-FIP model code 1990, Thomas Telford, London; 1993.
64. ACI, A. 2014. 318–14. *Building Code Requirements for Structural Concrete, American Concrete Institute, Farmington Hills, Michigan*.
65. ACI 363R-92. State-of-the-art report on high-strength concrete. ACI committee report 363. American Concrete Institute, Detroit, 363R1–363R55; 1992.
66. Nihal Arioglu, Z. Canan Girgin, and Ergin Arioglu.,, "Evaluation of Ratio between Splitting Tensile strength and Compressive Strength for Concretes up to 120 MPa and its Application in Strength Criterion," *ACI Materials Journal.*, 103 91), pp19 - 24, 2006.
67. M. Albitar, M.M. Ali, P. Visintin, M. Drechsler, Effect of granulated lead smelter slag on strength of fly ash-based geopolymer concrete. Constr. Build. Mater. **83**, 128–135 (2014). https://doi.org/10.1016/j.conbuildmat.2015.03.009
68. G. Lavanya, J. Jegan, Evaluation of relationship between split tensile strength and compressive strength for geopolymer concrete of varying grades and molarity. Int. J. Appl. Eng. Res **10**(15), 35523–35527 (2015)
69. Jaber, A., Gorgis, I., & Hassan, M. (2018). Relationship between splitting tensile and compressive strengths for self-compacting concrete containing nano-and micro silica. In *MATEC Web of Conferences* (Vol. 162, p. 02013). EDP Sciences.
70. A.A. Ramezanianpour, A. Pilvar, M. Mahdikhani, F. Moodi, Practical evaluation of relationship between concrete resistivity, water penetration, rapid chloride penetration and compressive strength. Constr. Build. Mater. **25**(5), 2472–2479 (2011)
71. R.A. Medeiros-Junior, M.G. Lima, M.H.F. Medeiros, L.V. Real, Investigation of the compressive strength and electrical resistivity of concrete with different types of cement. J. ALCONPAT **4**, 113–128 (2014)
72. D.H. de Bem, D.P.B. Lima, R.A. Medeiros-Junior, Effect of chemical admixtures on concrete's electrical resistivity. Int. J. Build. Pathol. Adapt. **36**(2), 174–187 (2018)
73. C.C Araújo, & G.R Meira, Correlation between concrete strength properties and surface electrical resistivity. Revista IBRACON de Estruturas e Materiais, 15 (2021)
74. C. Andrade, R. D'andrea, The electrical resistivity as a control parameter of the concrete and its durability. J. ALCONPAT **1**, 90–98 (2011)
75. X. Lu, F. Tong, X. Zha, G. Liu, Equivalent method for obtaining concrete age on the basis of electrical resistivity. Sci. Rep. **11**(1), 1–12 (2021)
76. K.P.V. Robles, J.J. Yee, S.H. Kee, Electrical resistivity measurements for nondestructive evaluation of chloride-induced deterioration of reinforced concrete—a review. Materials **15**(8), 2725 (2022)
77. J. Priou, Y. Lecieux, M. Chevreuil, V. Gaillard, C. Lupi, D. Leduc, F. Schoefs, In situ DC electrical resistivity mapping performed in a reinforced concrete wharf using embedded sensors. Constr. Build. Mater. **211**, 244–260 (2019)
78. R.S. Raj, G.P. Arulraj, N. Anand, B. Kanagaraj, E. Lubloy, M.Z. Naser, Nanomaterials in geopolymer composites: a review. Develop. Built Environ. (2022). https://doi.org/10.1016/j.dibe.2022.100114
79. Q. Fu, W. Xu, X. Zhao, M. Bu, Q. Yuan, D. Niu, The microstructure and durability of fly ash-based geopolymer concrete: a review. Ceram. Int. **47**(21), 29550–29566 (2021). https://doi.org/10.1016/j.ceramint.2021.07.190
80. H.M. Khater, Effect of nano-silica on microstructure formation of low-cost geopolymer binder. Nanocomposites **2**(2), 84–97 (2016). https://doi.org/10.1080/20550324.2016.1203515
81. P.S. Deb, P.K. Sarker, S. Barbhuiya, Effects of nano-silica on the strength development of geopolymer cured at room temperature. Constr. Build. Mater. **101**, 675–683 (2015). https://doi.org/10.1016/j.conbuildmat.2015.10.044
82. M. Ibrahim, M.A.M. Johari, M. Maslehuddin, M.K. Rahman, Influence of nano-SiO2 on the strength and microstructure of natural pozzolan based alkali activated concrete. Constr. Build. Mater. **173**, 573–585 (2018). https://doi.org/10.1016/j.conbuildmat.2018.04.051
83. K. Gao, K.L. Lin, D. Wang, C.L. Hwang, B.L.A. Tuan, H.S. Shiu, T.W. Cheng, Effect of nano-SiO2 on the alkali-activated characteristics of metakaolin-based geopolymers. Constr. Build. Mater. **48**, 441–447 (2013). https://doi.org/10.1016/j.conbuildmat.2013.07.027
84. K. Gao, K.L. Lin, D. Wang, H.S. Shiu, C.L. Hwang, B.L.A. Tuan, T.W. Cheng, Thin-film-transistor liquid-crystal display waste glass and nano-SiO2 as substitute sources for metakaolin-based geopolymer. Environ. Prog. Sustain. Energy **33**(3), 947–955 (2014). https://doi.org/10.1002/ep.11868
85. Q. Li, H. Xu, F. Li, P. Li, L. Shen, J. Zhai, Synthesis of geopolymer composites from blends of CFBC fly and bottom ashes. Fuel **97**, 366–372 (2012). https://doi.org/10.1016/j.fuel.2012.02.059
86. H. Assaedi, F.U.A. Shaikh, I.M. Low, Characterizations of flax fabric reinforced nanoclay-geopolymer composites. Compos. B Eng. **95**, 412–422 (2016). https://doi.org/10.1016/j.compositesb.2016.04.007
87. H. Assaedi, F.U.A. Shaikh, I.M. Low, Effect of nano-clay on mechanical and thermal properties of geopolymer. J. Asian Ceram. Soc. **4**(1), 19–28 (2016). https://doi.org/10.1016/j.jascer.2015.10.004